HSA

UNIVERSIDADE Đ COIMBRA

Andreia Filipa Da Costa Tuna

INTERACTION BETWEEN ALBUMINS AND CLINICALLY APPROVED HIV-TRANSCRIPTASE REVERSE INHIBITORS

Setembro de 2022

Andreia Filipa Da Costa Tuna

INTERACTION BETWEEN ALBUMINS AND CLINICALLY APPROVED HIV-TRANSCRIPTASE REVERSE INHIBITORS

Dissertação apresentada para provas de Mestrado em Química Medicinal

Orientador: Professor Doutor Carlos Serpa
Coorientador: M.Sc. Otávio Augusto Chaves

Setembro de 2022

Universidade de Coimbra

ACKNOWLEDGMENTS

TABLE OF CONTENTS

LIST OF FIGURES

FIGURES OF APPENDIX

LIST OF TABLES

TABLES OF APPENDIX

ABBREVIATIONS

τ - Lifetime.
3TC - Lamivudine.
AIDS - Immunodeficiency syndrome.
AGEs - Advanced glycation end products.
Arg - Arginine.
ART - Antiretroviral therapy.
AZT - Zidovudine
AZT-MP - Zidovudine monophosphate.
BSA - Bovine serum albumin.
CCDC - Cambrigde Crystallographic Data Center.
CMC - Carboxylmethyl-cysteine-cysteine.
COP - Colloid osmotic pressure.
CQP - Chloroquine diphosphate.
Cys - Cysteine.
DFT - Density functional theory.
DRV - Darunavir.
DTG - Dolutegravir.
EGV - Elvitegravir.
Env - Viral envelope.
E-TP - Emtricitabine 5´-triphosphate.
FDA - Food and drug administration.
FCT - Emtricitabine.
g-HSA - Glycated human serum albumin.
Gp - Glycoprotein.
gRNA - Genomic RNA.
HSA - Human serum albumin.
HIV - Human immunodeficiency virus.
IBUP - Ibuprofen.
IRF - Instrumental response function.
ITC - Isothermal titration calorimetry.
K/K_b - Binding constant.
K_{diff} - Diffusion rate constant.
K_{sv} - Stern-Volmer constant.
K_q - Quenching constant.
Lys - Lysine.
MD - Molecular docking.
mRNA - Messenger RNA.
N - Number of binding sites.
Nef - Negative regulatory factor.
NNRTIs - Non-nucleoside reverse transcriptase inhibitors.
NRTIs - Nucleoside reverse transcriptase inhibitors.

PBS - Phosphate-buffered saline.

PI - Protease inhibitor.

PLWHIV - People living with HIV.

PS - Phenelzine sulfate.

RAL - Raltegravir.

Rev - Regulator of virion.

RMSD - Room mean square deviation.

RT - Transcriptase reverse.

SIV - Simian immunodeficiency virus.

SIVcpz - SIV from chimpanzees.

SIVsm - SIV from sooty mangabeys.

SSF - Steady-state fluorescence.

TAF - Tenofovir Alafenamide.

Tat - Trans-activator of transcription.

TCSPC - Time-correlated single photon counting.

TDF - Tenofovir Disoproxil Fumarate.

TFV - Tenofovir.

TFV-DP - Tenofovir diphosphate.

TRF - Time-resolved fluoprescence.

Trp - Triptophan.

vDNA - Viral DNA.

Vif - Viral infectivity factor.

Vpr - Viral protein R.

WAR - Warfarin.

ABSTRACT

The human immunodeficiency virus (HIV) is a lentivirus that belong to the class of retrovirus. Its genome is composed of two homologous copies of ribonucleic acid (gRNA) which will be converted to deoxyribonucleic acid (DNA) by action of reverse transcriptase (RT) enzyme. Thus, one of the ways to decrease the virus replication into the host cells is the inhibition of RT processability and to achieve this goal different drugs were clinically approved by Food and Drug Administration (FDA), however, there are lack of biophysical characterization on its interaction with some specific proteins, such as globular proteins present in the human bloodstream.

One of the objectives of this project is evaluate the interaction between six clinically approved RT inhibitors: tenofovir (TFV) and its two prodrugs tenofovir disoproxil fumarate (TDF) and tenofovir alafenamide (TAF); emtricitabine (FCT), lamivudine (3TC), and zidovudine (AZT) with serum albumins, e.g., human serum albumin (HSA) and its glycated form, due to the distribution of these drugs throughout the body has not yet been reported in the literature. Theoretical calculations (molecular docking), spectroscopic techniques (UV-Vis absorption, steady-state fluorescence and time-resolved fluorescence), and heat measurements (isothermal titration calorimetry) were used.

Once that the interaction between the antiretrovirals and albumin has been studied, the same experience will be made using glycated human serum albumin (g-HSA) to establish whether there is any difference in the interaction between the antiretrovirals and the two albumins (non-glycated and glycated). The glycated albumin is present in people who suffer from diabetes, one of the pathologies with the most cases in the world. To date, there is not much information on the interaction of g-HSA with drugs, so the study of these antiretrovirals with g-HSA would be very useful to establish whether the structural modifications in the glycated albumin will favor or not an interaction.

RESUMO

O vírus da imunodeficiência human (VIH) é um lentivírus que pertencente à família dos retrovírus. O seu genoma é constituído por duas cópias homólogas de ácido ribonucleico (ARNg) que é convertido a ADN pela ação da enzima transcriptase reversa (TR). Portanto, uma das formas para diminuir a replicação do vírus é a inibição da processabilidade da TR na célula hospedeira, e para atingir esse objetivo diferentes drogas foram clinicamente aprovadas pelo *Food and Drug Administration* (FDA), no entanto, há uma ausência de caracterização biofísica de sua interação com proteínas específicas, como proteínas globulares presentes na corrente sanguínea.

Um dos objetivos deste projeto é avaliar a interação entre seis inibidores clinicamente aprovados para TR: tenofovir (TFV) e dois de seus pró-farmacos tenofovir disoproxil fumarato (TDF) e tenofovir alafenamida (TAF); emtricitabine (FCT), lamivudine (3TC) e zidovudine (AZT) com proteínas séricas, por exemplo albumina do soro humano e sua forma glicada, devido a que não foi reportado na literatura a distribuição destes fármacos pelo organismo. Serão usados cálculos teóricos (docking molecular), técnicas espectroscópicas (absorção no UV-Vis, fluorescência no estado estacionário e fluorescência resolvida no tempo) e medições de calor (calorimetria de titulação isotérmica).

Uma vez estudada a interação entre os antirretrovirais e a albumina, a mesma experiência será feita usando a albumina sérica humana glicada (g-HSA) de modo a estabelecer se existe alguma diferença na interação entre os antirretrovirais e as duas albuminas (não glicada e glicada). A albumina glicada está presente em pessoas quem padecem diabetes, uma das patologias com mais casos no mundo. Ate à data, não existe muita informação sobre a interação da g-HSA com medicamentos, pelo que o estudo destes antirretrovirais com a g-HSA seria muito útil para estabelecer se as modificações estruturais que sofre a albumina ao ser glicada vai favorecer ou não a que exista uma interação.

CHAPTER 1: INTRODUCTION

1.1. HIV

  Lentivirus is a class of retrovirus that cause chronic and deadly diseases characterized by the slow time course of infection in the host [1]. The genome of retroviruses is a dimer composed by two homologous copies of genomic RNA (gRNA) of positive polarity [2] The gRNA molecules are replicated through a formation of viral DNA by retro-transcription. This process is regulated by a DNA polymerase dependent of RNA, known as reverse transcriptase [3].

  The human immunodeficiency virus (HIV), one of the most known and spread lentivirus, has already infected about 33.9 - 43.8 million people until 2021, and only in 2021 increased the number of people living with HIV (PLWHIV) by about 1.1 – 2.0 million [4] This virus can be divided into HIV type 1 or type 2 (HIV-1 and HIV-2, respectively) [5]. Comparing HIV-1 and HIV-2, the first one has the highest replication capacity into infected cells and impacts faster the immune system of the host. Overall, there are more PLWHIV type 1 than type 2, e.g., in a total of 327,700 PLWHIV in the United States of America from 2010 until 2017, about 327,502 (99,94%) are infected with type 1 (**Figure 1**). The remaining 0.06% (198 PLWHIV) were classified as monoinfected with type 2 ($n = 102$), with both types at the same time ($n = 11$), or unconfirmed type ($n = 85$) [6,7]. Both types of HIV were introduced into human species after spillover by direct contact with infected animals, more specific with the progenitor virus simian immunodeficiency (SIV, from sooty mangabey and chimpanzee, that originated HIV-2 and HIV-1, respectively) [5,6].
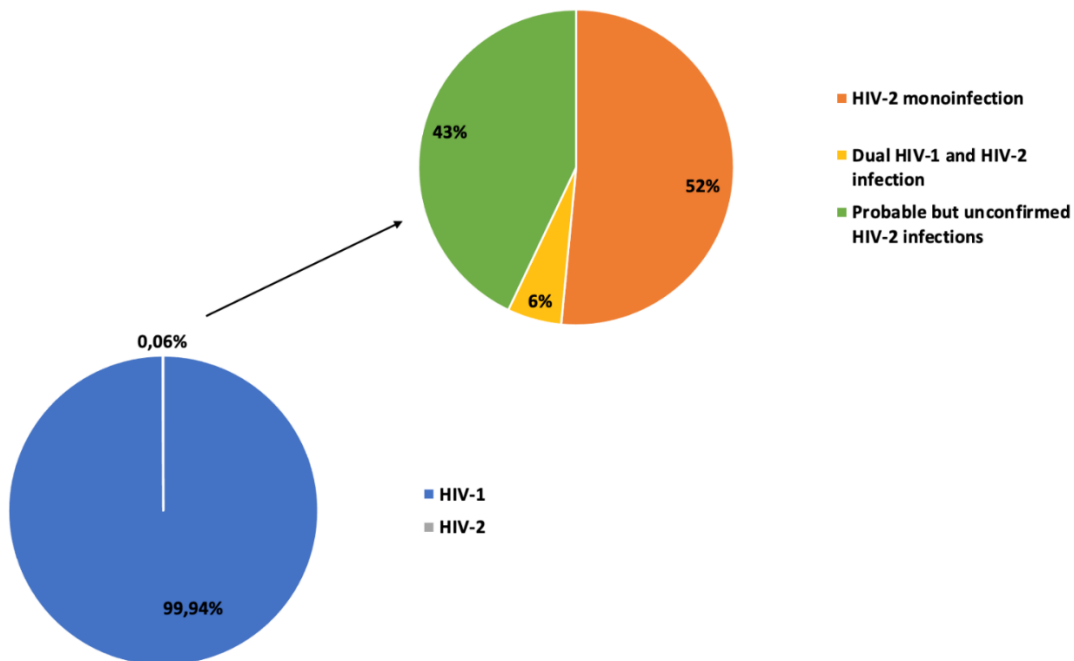
Figure 1. Number of PLWHIV type 1 and 2 in the United States from 2010 until 2017 [7].

The infection by HIV is divided in three phases: in the first phase or severe infection, the amount of virus in the human blood is very high (can appear symptom or not), while in the second phase or chronic infection by HIV (or asymptomatic phase), the number of viruses in the human blood decreases and its production from the target cells is very slow. At the end of this phase the viral charge is very high and the number of CD4 (or T) cells is reduced, e.g., in a non-infected person the number of CD4 cells is 500-1,200 per cubic millimeter, while in PLWHIV the number of CD4 cells is 250-500 per cubic millimeter. Finally, in the third phase, the acquired immunodeficiency syndrome (AIDS) is developed, and the number of CD4 cells are about 200 or lower per millimeter. In this sense, the immune system was drastically negative impacted, and it implicated the development of different pathogens. With the advances of treatment in this disease, is not commonly that infected people reach the last phase [6,8].

From a structural point of view (**Figure 2**), the HIV has a lipid envelope in which embedded the gp41, trimeric transmembrane glycoprotein, to which the surface glycoprotein gp120, essential to the attachment with the surface of other cells before the invasion is attached; this heterodimer form the viral envelope (Env) protein [9]. The matrix protein, p17, is involved in most stages of the cycle of the retrovirus. It participates in the early stages of virus replication as well as in gRNA targeting to the plasma membrane, incorporation of the envelope into virions and particle assembly [10]. More internal is the capsid protein, an essential structure that protects the reverse transcription complex from restriction factors [11]. Another structural protein is the nucleocapsid protein, essential to viral replication; recent studies have demonstrated reverse transcription occurs inside the fully intact viral capsid and that the timing of reverse transcription and uncoating are correlated [12]. The HIV has three viral enzymes: reverse transcriptase, integrase, and protease. The reverse transcriptase contains both DNA polymerase and RNase H activities to convert the viral genomic RNA to viral DNA (vDNA) in infected host cells [13]. The integration of vDNA into cellular DNA, an essential step in the replication cycle, is regulated by integrase [14]. HIV protease is required for viral infectivity since mutation of the catalytic residues as well as chemical inhibition of the enzyme leads to the production of immature noninfectious viral particles [15].

Other elements present in the HIV structure are five accessory proteins: viral infectivity factor (vif), viral protein R (vpr), negative regulatory factor (nef), regulator of virion (rev), and trans-activator of transcription (tat). The vif is required for HIV replication in cells that are termed nonpermissive, which include lymphocytes and macrophages and some leukemic T-cell lines, however, it is irrelevant for viral replication in cells that are termed permissive, which include other leukemic T-cell lines [16]. Vpr plays several important functions in the early stages of the viral lifecycle. This protein has a variety of biological functions, including interaction with and translocation of the HIV pre-integration complex through the nuclear pore, coactivation of steroid hormone receptors, modulation of apoptosis and induction of host cell cycle arrest at the G2/M transition phase

of the cell cycle, and stimulation of viral gene expression [17,18,19]. Nef established the host cell environment suitable for viral replication and pathogenesis and facilities the progression of the infection into disease, is critical for pathogenesis [20]. Rev mediates the appearance of unspliced and singly spliced RNA in the cytoplasm by facilitating the nuclear export of the RNA [21]. Tat regulates the expression of cellular genes, modulating key pathways and mechanisms to generate an environment that favors the production and spread of HIV to promoting viral transcription [22].
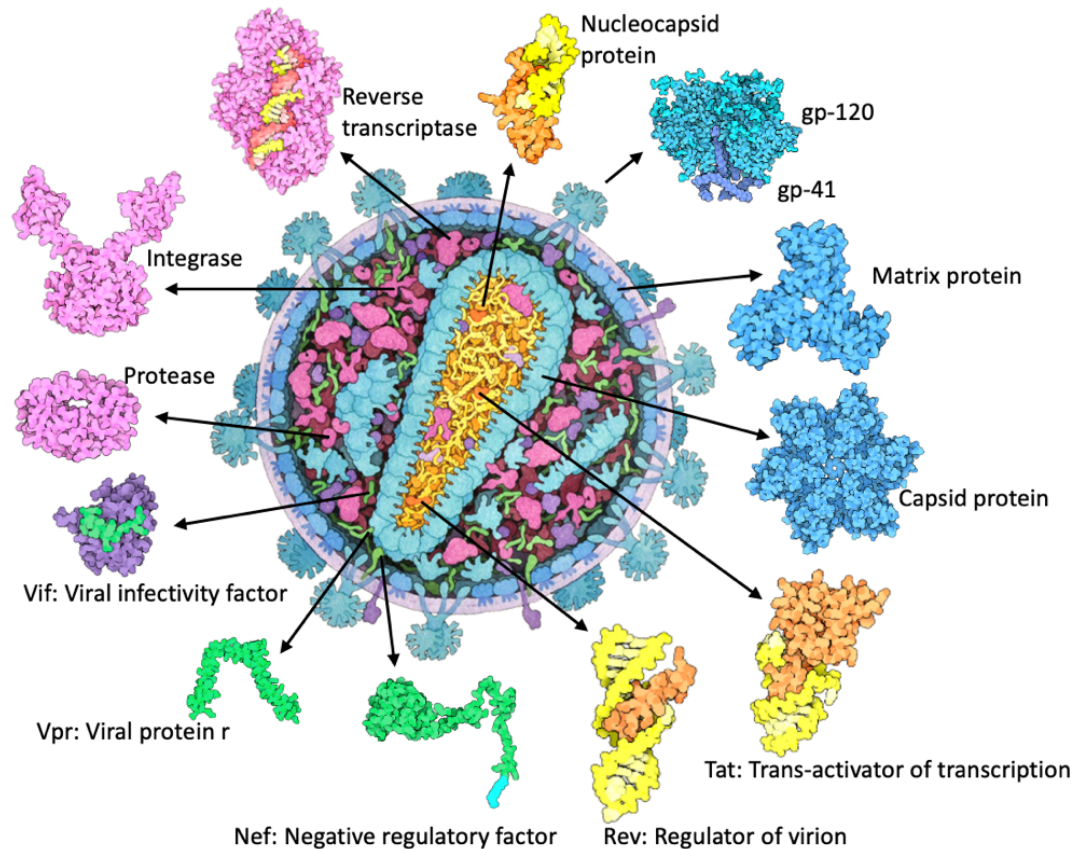
Figure 2. The main proteins which compose the HIV structure. Adapted from Protein Data Bank (PDB) [23].

The HIV replication cycle (**Figure 3**) can be divided in nine main steps: binding, fusion, reverse transcription, integration, transcription, translation, assembly, budding/release, and maduration. The first and second steps play a major role in determining viral tropism and the ability of HIV to impact the human immune system. This begins with adhesion of virus to the host cell, regulated by the viral envelope (Env) protein. After, the Env binds to its primary receptor (superficial protein from CD4) there is a conformational change in Env structure, allowing coreceptor binding. To finish this step, there is the fusion of the cell and viral membranes with subsequent delivery of the viral core into the cytoplasm [24]. In the third step (reverse transcription) there is the participation of reverse

transcriptase (RT) to convert vRNA into vDNA [25]. The integration of vDNA into the host cell chromosome is the next step in the presence of integrase (IN) and other proteins as a high-molecular-weight nucleoprotein complex that is later transported to the nucleus for subsequent integration [26]. After integration of the vDNA, it is necessary the transcription, and the formation of mRNA [27]. The mRNA is exported to the cytoplasm and translated to produce rev, tat, and nef [28]. Then, the assembly at the plasma membrane occurs and the virion is generated. To finish the cycle, the virion crosses the plasma membrane and obtain its lipid envelope, this step is called budding and after it, the virion maturates (action of proteases) to becomes infectious [29].
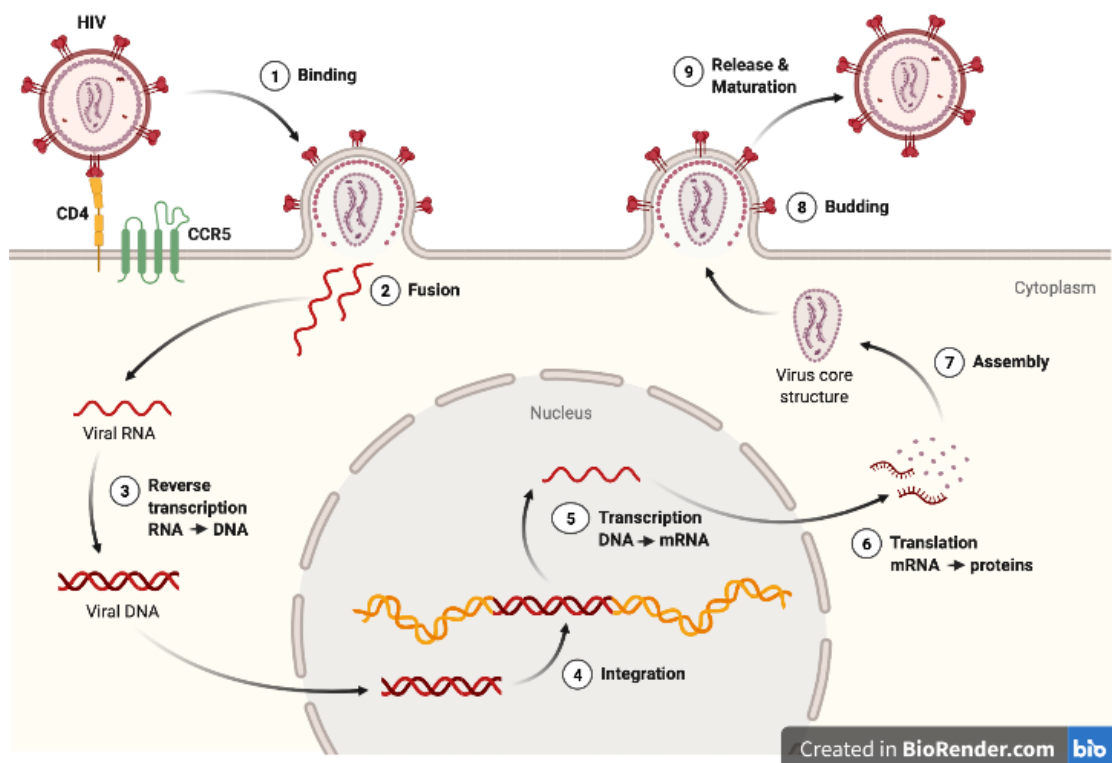
Figure 3. The HIV replication cycle [30].

1.2. HIV ANTIRETROVIRALS

Antiretroviral therapy (ART) is considered one of the effective ways to decrease and increase the number of HIV and CD4 cells, respectively, in the bloodstream. If the quantification of HIV is less than 200 virus copies per milliliter of blood, is considered the virus as indetectable, meaning that the immune system is not more damaged by the viruses and there is a very low probability of transmission [31].

The ART involves a combination of drugs - usually three different drugs of at least two different classes of inhibitors. The HIV antiretrovirals drugs can be divided into five groups [31]:

-Protease inhibitors (PI): is one of the most important components in the combinatory therapy. The therapy based in this group has a lower level of resistance compared with other groups. However, the secondary effects associated with PI is very high, that can be resulted from drug-drug interaction or overdose [32,33]. Darunavir, amprenavir, and ritonavir (**Figure 4**) are some examples of PI clinically approved by Food and Drug Administration (FDA).
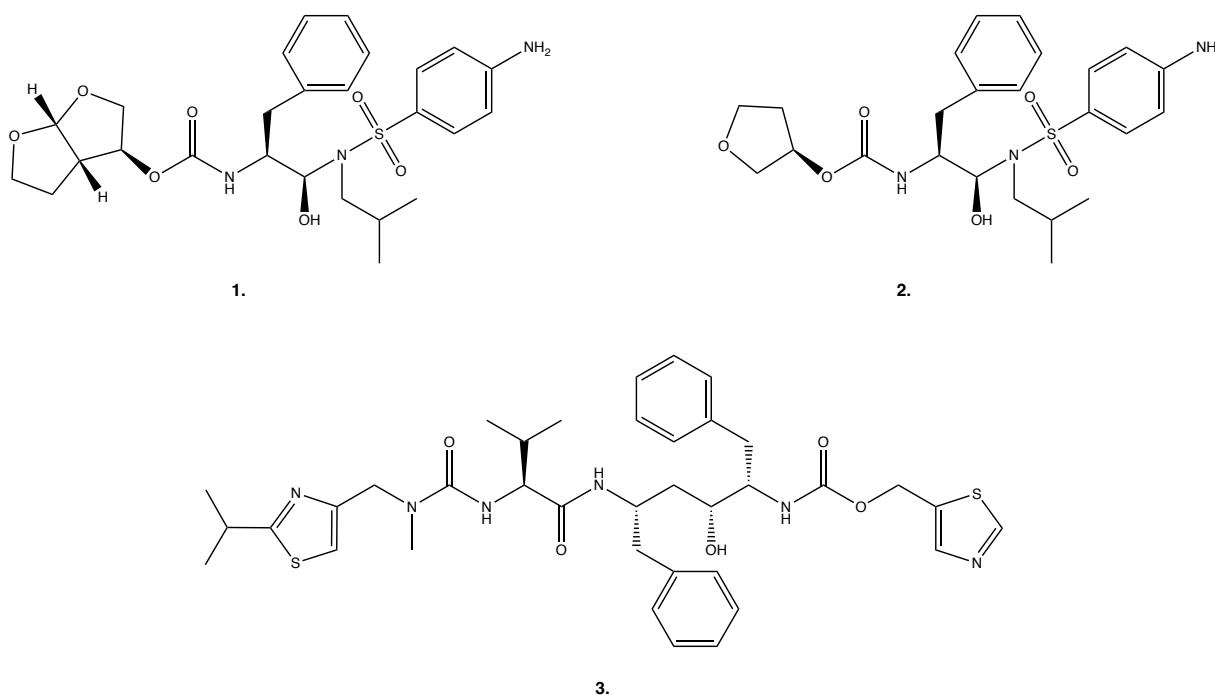
Figure 4. Chemical structure of protease inhibitors (PI) darunavir (**1**), amprenavir (**2**), and ritonavir (**3**).

- Entry inhibitors: as the entry of HIV into target cells is a complex, multi-step process, the effort to identify pharmacological agents that can interfere with entry has resulted in a heterogeneous group of compounds that act at multiple stages of the entry process and have distinct mechanisms of action. Generally, the

group of entry inhibitors can be subdivided into classes of agents that act at different stages: attachment and CD4 binding, coreceptor binding, or fusion. Today, only antagonists that block CCR5 (key cell-surface receptor for HIV) binding, and fusion (**Figure 5**) have been approved by FDA [34]. Enfuvirtide is a fusion inhibitor that binds to HIV-1 gp41, interrupting the fusion reaction and preventing the virus from infecting the host cell, while maraviroc is a CCR5 inhibitor [35, 36].

1.

2.
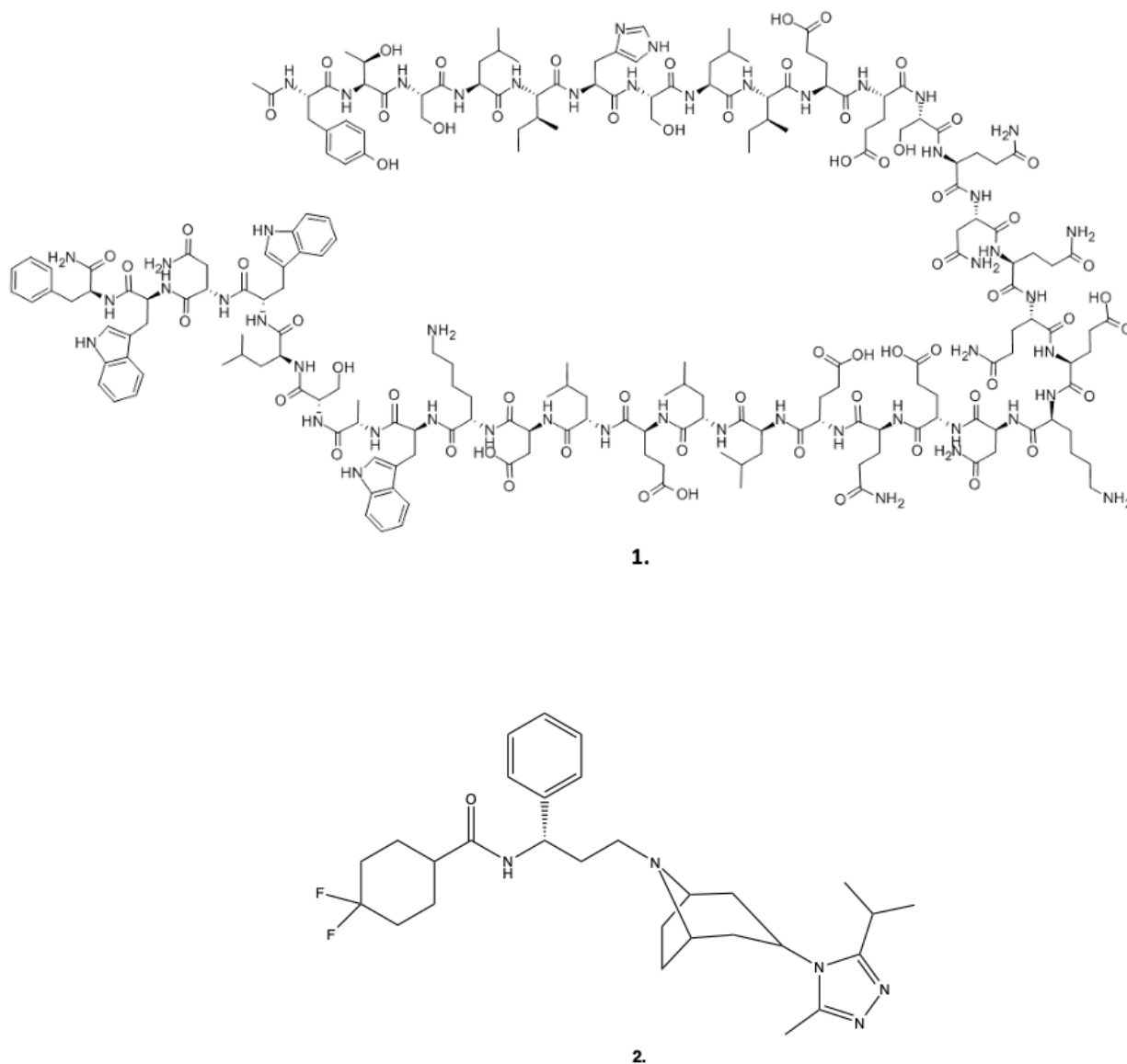
Figure 5. Chemical structure of entry inhibitors enfuvirtide (**1**) and maraviroc (**2**).

-Integrase inhibitors: Represent one of the most important advances in HIV care. The integrase is necessary for integration of vDNA into the host cell chromosomal DNA, a step that is critical to establish persistent HIV infection. Dolutegravir (DTG), elvitegravir (EGV), and raltegravir (RAL) (**Figure 6**) are some examples of integrase inhibitors clinically approved by FDA [37].
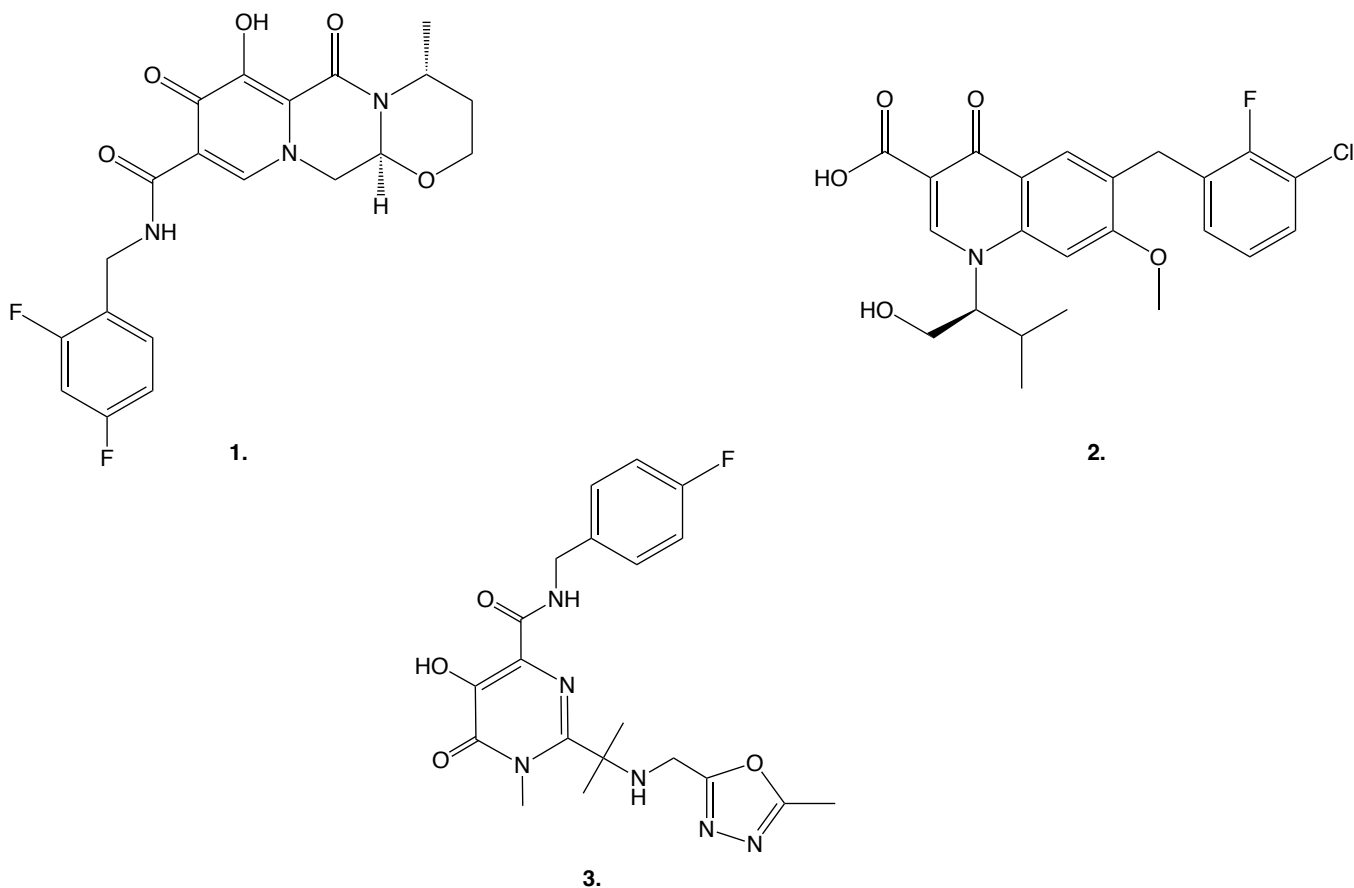
Figure 6. Chemical structure of integrase inhibitors dolutegravir (**1**), elvitegravir (**2**), and raltegravir (**3**).

-Reverse transcriptase inhibitors: These antiretrovirals can be divided in two subgroups:

1. Non-nucleoside reverse transcriptase inhibitors (NNRTIs). The NNRTIs bind in a hydrophobic pocket of the reverse transcriptase close to the active site. This interaction creates a new spatial configuration of the substrate-binding site, reducing the polymerase processability. The interactive amino acid residues of HIV-1 and HIV-2 RT to NNRTIs are different and for this reason NNRTIs is ineffective to HIV-2 [38, 39]. Some examples of these subgroups of antiretrovirals that are clinically FDA-approved are doravirine, efavirenz, and rilpivirine (**Figure 7**).
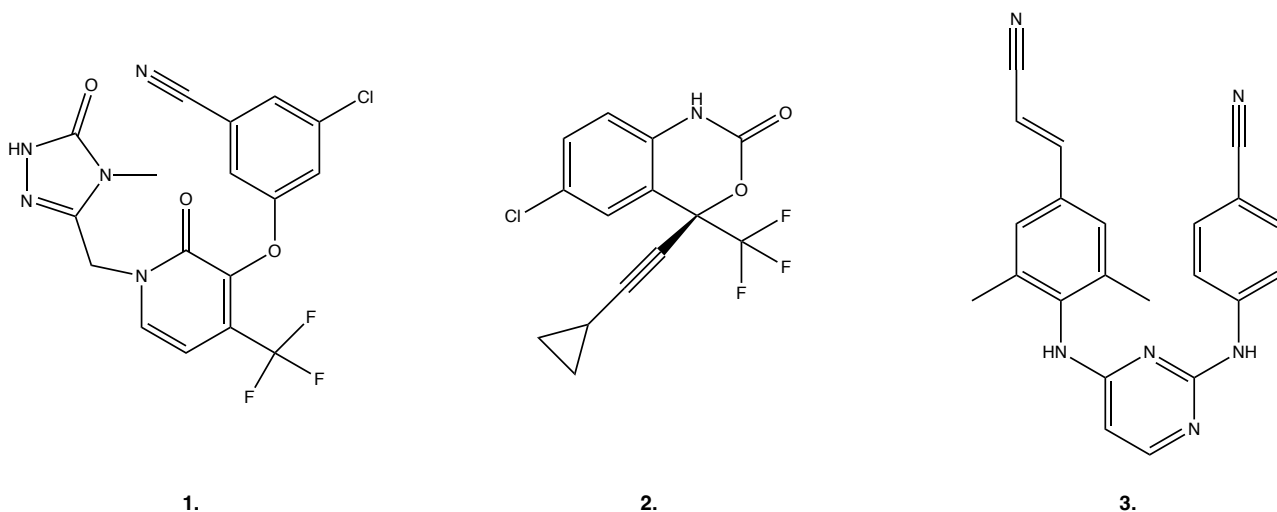
Figure 7. Chemical structure of non-nucleoside reverse transcriptase inhibitors (NNRTIs) doravirine (**1**), efavirenz (**2**), and rilpivirine (**3**).

2. Nucleoside reverse transcriptase inhibitors (NRTIs). These inhibitors act directly in the active site of the enzyme, being used as building blocks to the vDNA (inhibit the elongation of vDNA). There are six main clinically FDA-approved NRTIs: tenofovir (TFV), tenofovir disoproxil fumarate (TDF), tenofovir alafenamide (TAF), emtricitabine (FCT), lamivudine (3TC), and zidovudine (AZT).

   o TFV is a nucleotide analogue of adenosine monophosphate and an effective and widely drug used to treat HIV. Its active metabolite, tenofovir diphosphate, competes with natural deoxyadenosine triphosphate for the active binding site of reverse transcriptase. Incorporation of tenofovir diphosphate into vDNA results in chain termination, since tenofovir diphosphate lacks the hydroxyl groups in the 3′-position, which acts as the point of attachment for the next deoxyribonucleoside triphosphate. Hence, reverse transcription, the key step in HIV proliferation, is inhibited (**Figure 8**) [40, 41]. However, tenofovir has a bioavailability limited due to their negative charges in the phosphoryl group and a relatively low plasma stability, therefore, two prodrugs have been developed: TDF and TAF. TDF, a weak base prodrug of tenofovir is susceptible to hydrolysis by water and cellular esterases (**Figure 8**). The TDF permeates cells more rapidly than tenofovir due to its increased hydrophobicity, resulting in increased intracellular

accumulation of tenofovir diphosphate (TFV-DP, the active metabolite). TFV-DP levels are ~1000-fold higher in tenofovir DF-treated cells compared with tenofovir-treated cells and the tissue permeability of tenofovir DF is ≥10-fold higher than that of tenofovir [42]. On the other hand, TAF was identified as an alternate TFV prodrug to TDF that more efficiently loads HIV-target cells. TAF is 1000- and 10-fold more active against HIV *in vitro* than TFV or TDF, mainly due to its stability in biological matrices, inciuding plasma. The three tenofovir cross the membrane cellular for passive difussion; in the case of prodrugs, esterases are the responsables of hydrolised the ester bonds for form the tenofovir [43].
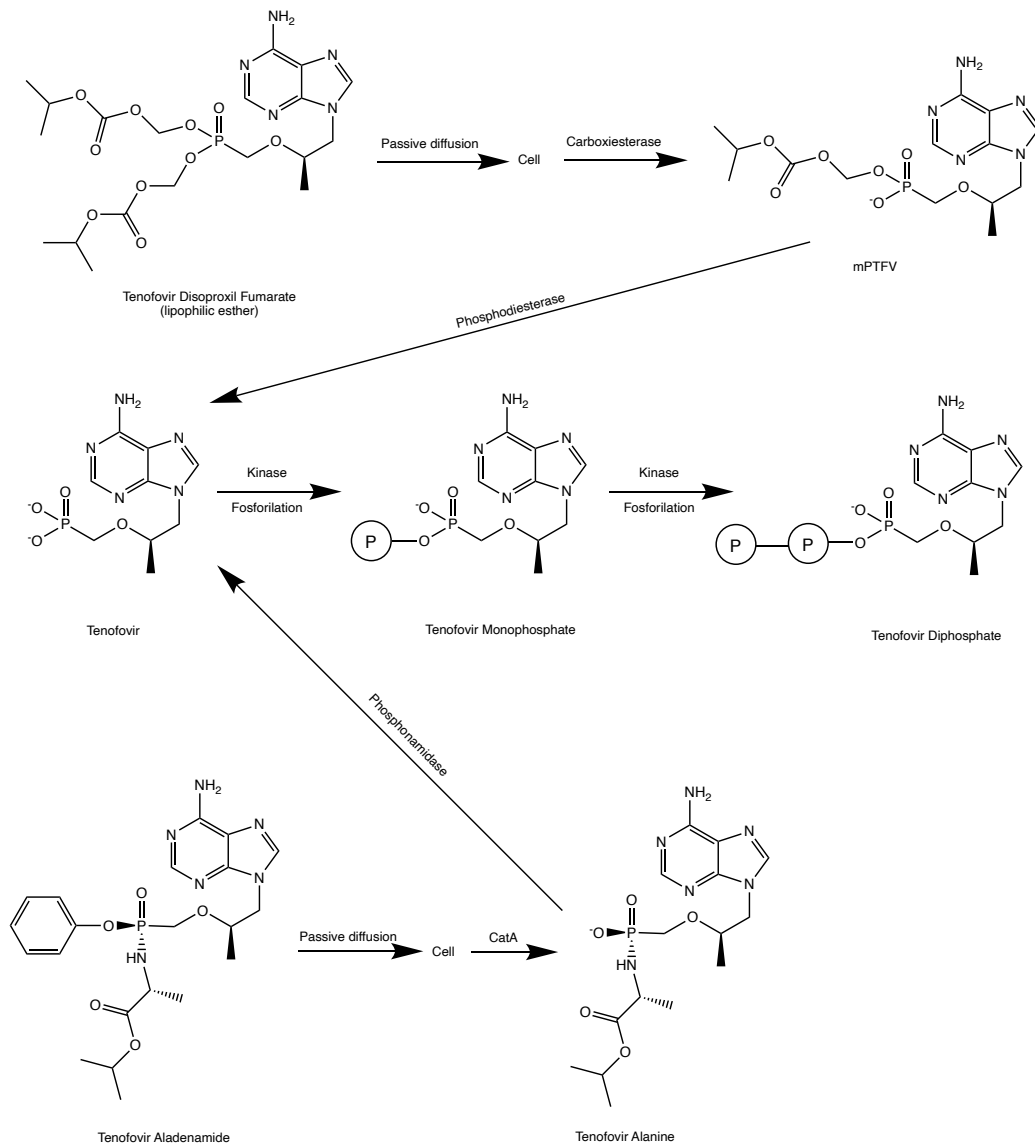
Figure 8. Mechanism of the drugs belonging to the class of tenofovir.

- o FCT is a pyrimidine nucleoside analogue and a prodrug that is phosphorylated intracellularl by 2´-deoxycytidine kinase into its active triphosphate form, emtricitabine 5´-triphosphate (E-TP) (**Figure 9a**). E-TP is incorporated by reverse transcriptase into the elongating proviral DNA chain leading termination of DNA synthesis through the inability of the next nucleotide to bind to E-TP at the 3´-position [44, 45]. The mechanism of FCT inhibition is a competitive inhibition between E-TP and the natural substrate deoxycytidine 5´-triphosphate [46].
- o 3TC is a nucleoside analogue of 2´-deoxycytidine that exerts its antiretroviral effects by acting as a DNA chain terminator. The active metabolite of 3TC is lamivudine 5´-triphosphate, and it´s formed from phosphorylation by intracellular kinases, 2´-deoxycytidine kinase, (**Figure 9b**) and competes with naturally occurring cytidine triphosphate for incorporation into DNA [47, 48].
- o AZT is structurally related to the endogenous nucleoside thymidine. AZT is phosphorylated by three kinases to form the active triphosphate, following the passive diffusion of the drug into target cell. The enzyme thymidine kinase is responsible for intracellular formation of AZT monophosphate (AZT-MP), after a thymidine kinase transforms AZT-MP in AZT diphosphate, and, the last step, is the formation of AZT triphosphate by the enzyme pyrimidine nucleoside diphosphate kinase (**Figure 9c**).The AZT mechanism of action involves the inhibition of action of thymidine incorporation into viral DNA by reverse transcriptase and subsequent DNA chain termination in HIV-cells, both of which are carried out by active form of the drug, zidovudine 5´-triphosphate [49] .
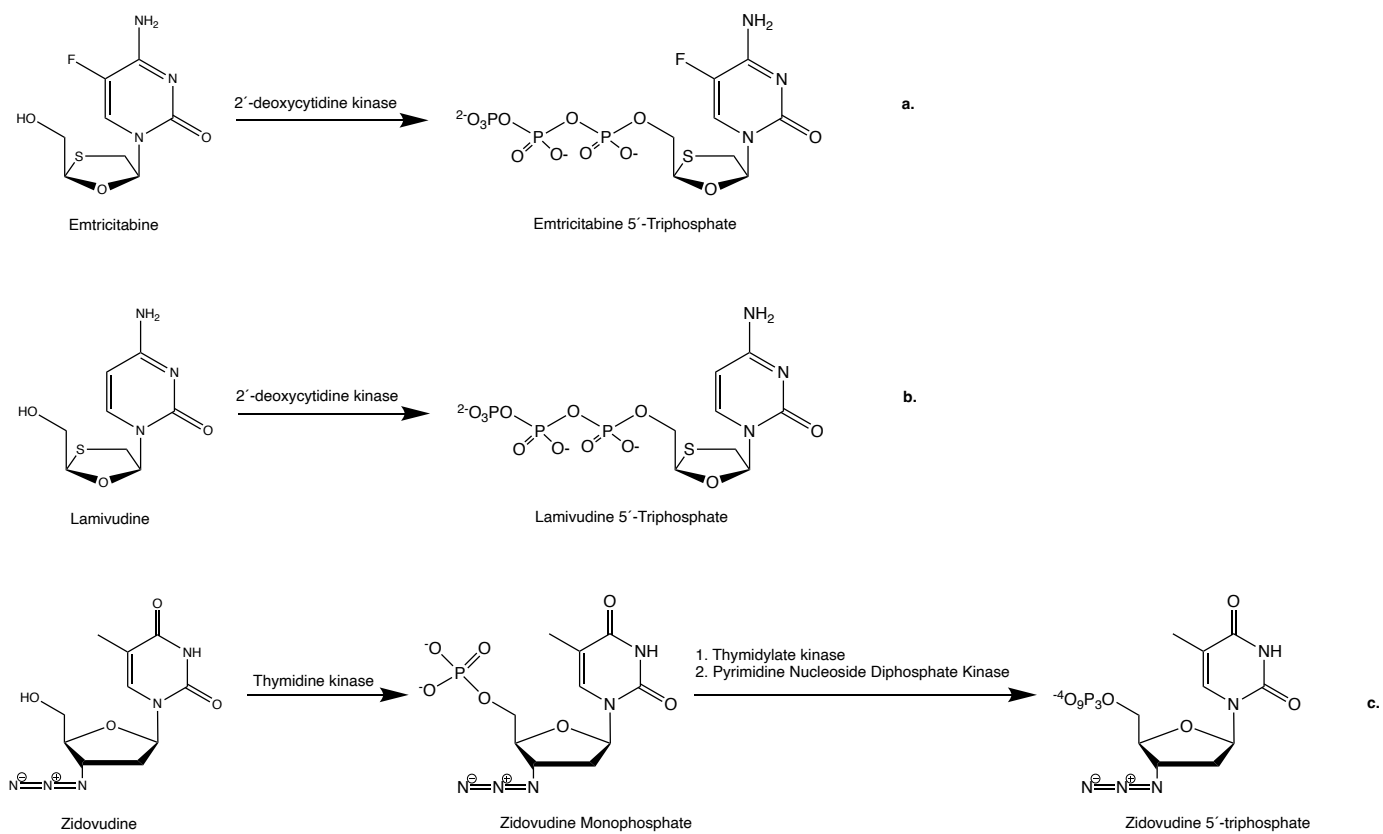
Figure 9. Mechanism of active metabolite formation to emtricitabine (**a**), lamivudine (**b**) and zidovudine (**c**).

1.3. SERUM ALBUMIN

The human serum albumin (HSA) is the most abundant globular protein in human plasma, being synthetized in the liver and exported as a single non-glycosylated chain in the blood, with a concentration of 5g/100mL (7.0×10^{-4} M). HSA is a monomeric multi-domain macromolecule that has many functions, acting as modulator of plasma oncotic pressure and carrier of a variety of endogenous (e.g., bilirubin, ions, and fatty acids) and exogenous (e.g., drugs) compounds to their specific targets [50, 51, 52, 53]. In healthy patients the role of the albumin to control the colloid osmotic pressure (COP) is more relevant than in critical patients, in this case the correlation is lower. In health patients the albumin contributes up to 80% of the normal COP (25 mmHg), it is caused by its high molecular weight and concentration in plasma compared to other proteins in the plasma [54]. The interaction between HSA and drugs is reversibly and the corresponding binding affinity is one of the major factors that determine the pharmacokinetic of the drug (absorption, distribution, metabolism, and elimination). If the binding affinity is low, the first step of pharmacokinetics, drug absorption, is not feasible. In the case that the binding affinity of bioactive substances to serum albumin is moderate, the absorption and the distribution of drugs to various tissues are feasible. The last option is a high binding affinity, in this case the absorption of drug is feasible, but the distribution to the required tissues is be limited to the stability of the complex which in turn adversely effects the pharmacokinetic of the drug [55].

Generally, the medium-sized organic anions, e.g., long-chain fatty acid, bilirubin, and haemitin, are the compounds that have a strong interaction with HSA. Substances with lower hydrophobic character, e.g., ascorbate and tryptophan bind weakly with HSA. The strongly negative charge of albumin might influence the degree of binding and for this reason the acid drugs have more preference to bound to other plasmatic proteins like α1-acid glycoprotein whereas the basic drugs prefer to bind to albumin [54].

From a structural point of view, the HSA structure consists of 585 amino acids that form a single polypeptide which contain 17 pair of disulfide bridges and one free cysteine. Turns and extended loops are features of HSA, a helical protein with heart shape. The HSA structure (**Figure 10a**) is divided in three domains: I (residues 1-194), II (195-385) and III (386-585), and each domain features two subdomains, the A with six α-helices and B, with four α-helices [51, 56]. For this 3D-structure, there are two main binding sites known as Sudlow´s sites: site I (a warfarin binding site), localized in the subdomain IIA, and site II (a benzodiazepine site), localized in the subdomain IIIA. Recently, a third pocket located in the subdomain IB (site III, a digitoxin binding site) has been reported as a feasible site for different types of drugs.

Some examples of compounds that preferentially bind to subdomain IIA are long chain fatty acids, some indole derivatives, organic compounds with

alicyclic ring moieties, dicarboxylic acids, and bulky heterocyclic with a negative charge. On the other hand, for site II (a hydrophobic pocket) has more tendency to interact with bilirubin, short chain fatty acids, some indole derivatives, steroids, and aromatic carboxylic acids with a negative charge located at the alpha carbon. Additionally, site I is more flexible than site II and its binding affinity is mainly driven by hydrophobic interactions, whereas site II involves a combination of hydrophobic, hydrogen binding, and electrostatic interactions [55]. Finally, for site III, some indole derivatives (e.g., diazepam), long chain fatty acids, and charged compounds are the main ligand to this region [57, 58, 59]. Based on intrinsic fluorescence of albumin, the HSA structure has only one tryptophan residue (Trp-214) which is localized in subdomain IIA [60, 61].

In terms of amino acid sequence, the bovine serum albumin (BSA) has a 76% of identity with HSA and its structure (**Figure 10b**) contains 583 amino acids, distributed in three homologous domains: domain I (residues 1-193), II (194-384), and III (385 -193) that are subdivided into two subdomains (A and B), connected by disulfide bonds, similarly to HSA. The BSA has two Trp residues, Trp-134 and Trp-213, one more Trp than in the HSA. The Trp-134 is localized in the subdomain IB, near the surface [56, 57, 60].
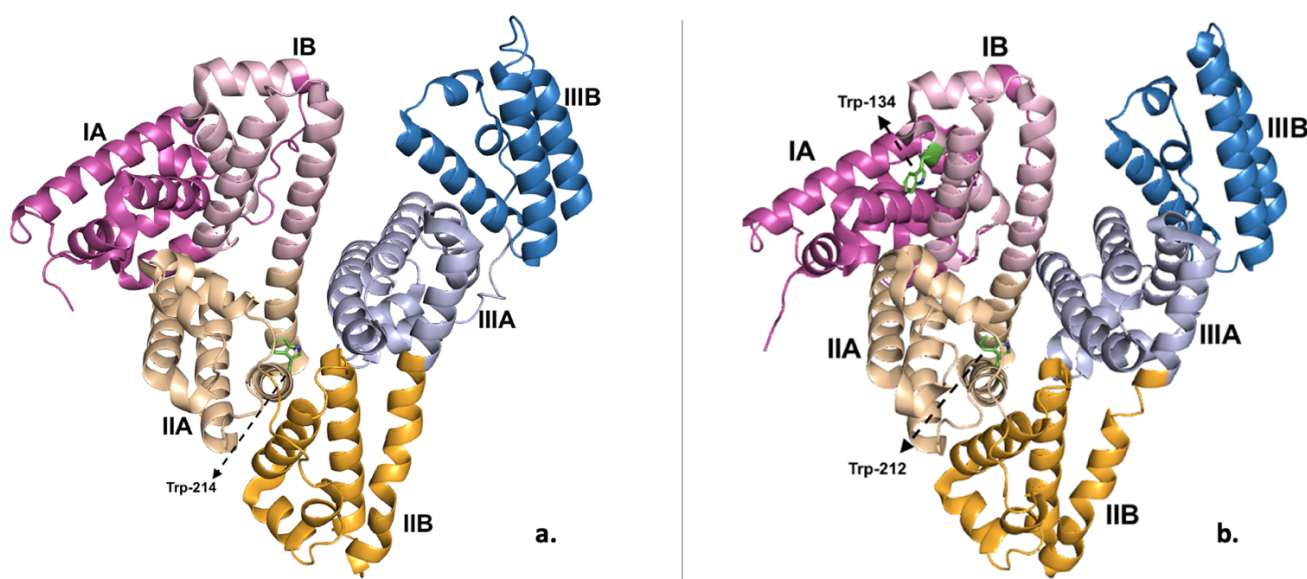
Figure 10. HSA (**a**) and BSA (**b**) structures. HSA structure is divided in three domains: I (residues 1-194), II (residues 195-385) and III (386-585); and, in six subdomains: IA/IB (rose/light rose), IIA/IIB (light orange /orange) and IIIA/IIIB (light blue/blue) with a Trp-residue, Trp-214, in the subdomain IIA or site I. BSA structure is also divided in three domains: I (residues 1-193), II (residues 194-384) and III (385-583); and, in six subdomains: IA/IB, IIA/IIB and IIIA/IIIB , with the same colors that the HSA structure, in this case there are two Trp-residues, Trp-134, in the subdomain IA or site III, and Trp-212 in the subdomain IIA or site I [56-60].

The concentration of glycated human serum albumin (g-HSA) in the bloodstream increases in diabetes patients. Diabetes occurs in 366 million people worldwide and it's described as a group of disorders that results from insulin deficiency and/or insulin resistance. Insulin is a peptide hormone secreted by β cells of the pancreatic islets and maintains normal blood glucose levels by facilitating cellular glucose uptake, regulating carbohydrate, lipid, and protein metabolism, and promoting cell division and growth thought its mitogenic effects. Insulin deficiency is defined as a pathological condition in which there is an inappropriate decrease in the rate at which β cells secreted insulin and insulin resistance is a pathological condition in which there is a shift in the dose-response curve such that the magnitude of the biological response to insulin decreased [60, 62, 63]. People with diabetes have the albumin glycated, and the glycation is one of the processes that is believed to affect the binding of drugs to HSA [64]. Glycation involves the non-enzymatic addition of reducing sugars and their reactive degradation products to primary or secondary amine groups on proteins. This process can occur for HSA and becomes more pronounced in diabetes when an elevated amount of glucose is present in the bloodstream. While an average individual has 6-13% of HSA in a glycated form, a person with diabetes may have 20-30% or more g-HSA in the circulation. Some of the primary modification sites for glycated HSA are at or near site I and II [64, 65].

- The non-enzymatic glycation (or simply glycation) does not involve the catalytic activity of glycosyltransferase. The reaction starts with a nucleophilic addiction reaction between the carbonyl group of reducing sugar and the amine group of the lysine, the arginine, or the N-terminus of the protein. The glucose is the main source of energy in the body and the primary raw material for this reaction in the body. The glycation can be divided in three steps (**Figure 11**): (1) the carbonyl group of reducing sugar undergoes a condensation reaction with the amine group of the protein to form a Schiff base that is unstable thermodynamically; (2) this unstable base, a intermediate product, is converted to a Amadori product that is relatively stable by a slow rearrangement, this two first steps are grouped into early stage glycation; (3) the product undergoes spontaneous reactions (i.e. dehydration, oxidation, rearrangement, and isomerization) that can generate various dicarbonyl compounds that react more strongly that the reducing sugars and more quickly to for the advanced glycation end products (AGEs), the advanced step glycation. Non-enzymatic glycosylation of albumin occurs at multiple residues such as arginine (Arg), lysine Lys), and cysteine (Cys), that are subjected to glycation mostly because of their high nucleophile properties. Lys-525 is considered to be predominant site of the human serum albumin *in vivo*

glycation which constitutes 30% of the overall glycation of the protein by glucose (another Lys residues, such as 199, 276, 281, 378, 439 and 545, have a lower participation than Lys-525 in overall glycation). Arg-410 is the predominant site of glycation (Arg-114, Arg-160, Arg-186, Arg-218 and Arg-428 are other residues that are involved in the glycation but not significantly). The thiol group of cysteine residues is powerful nucleophile, which can also be glycated in vitro by mehylglyoxal to give rise to AGEs such as S-carboxylmethyl-cysteine-cysteine (CMC). CMC occurrence in plasma from diabetic patients, suggest the involvement of Cys-34 in the glycation process (**Figure 12**). [62, 66, 67].

- Functional properties of HSA can be affected by the modifications induced by glycation, and have important implications for protein activity, folding, degradation, and cell function [66].

Early Stage Glycation (a)

Advanced Stage Glycation (b)
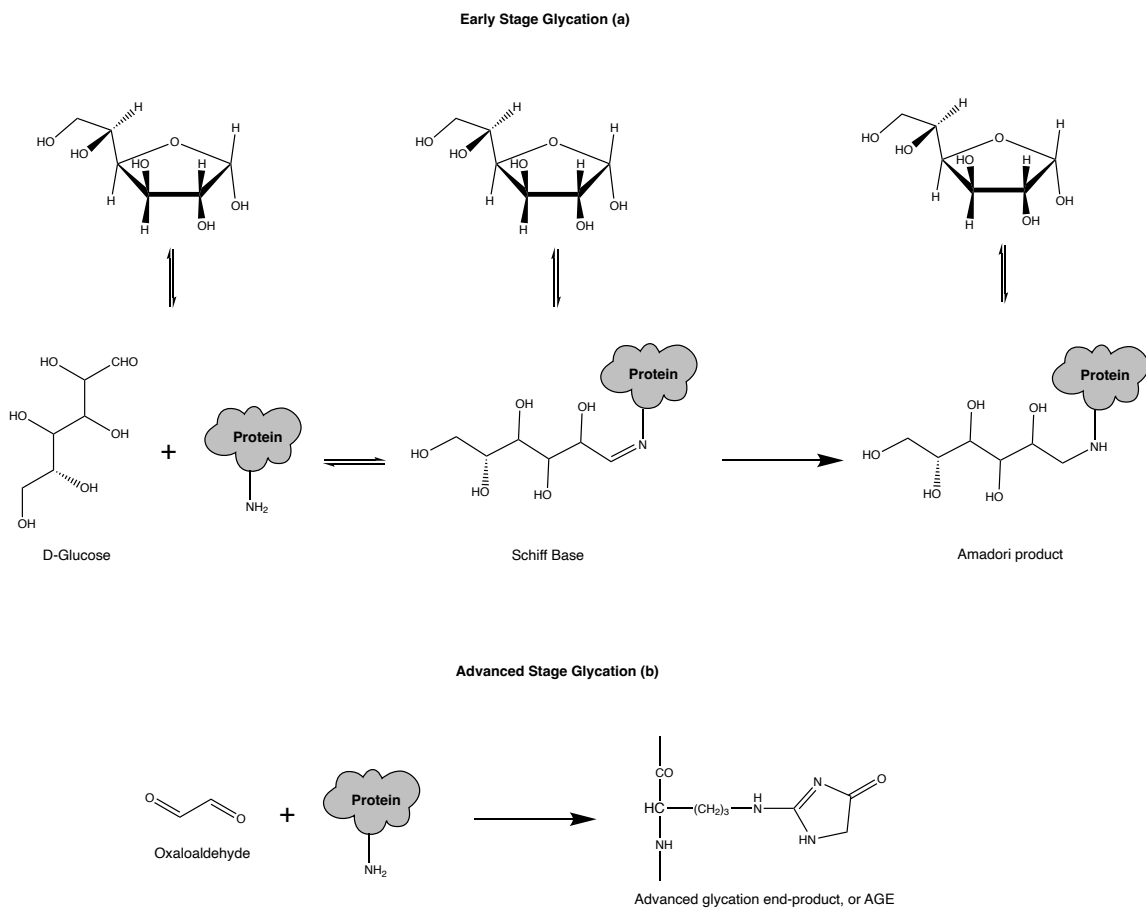
Figure 11. Glycation stages to albumin: (**a**) early-stage glycation, Schiff base (unstable intermediate) formation by the reaction between the reducing sugar and the amine group, the unstable intermediate its converts into Amadori product. (**b**) Formation of advanced-glycation end-products (AGEs) in the advanced stage glycation.[58].
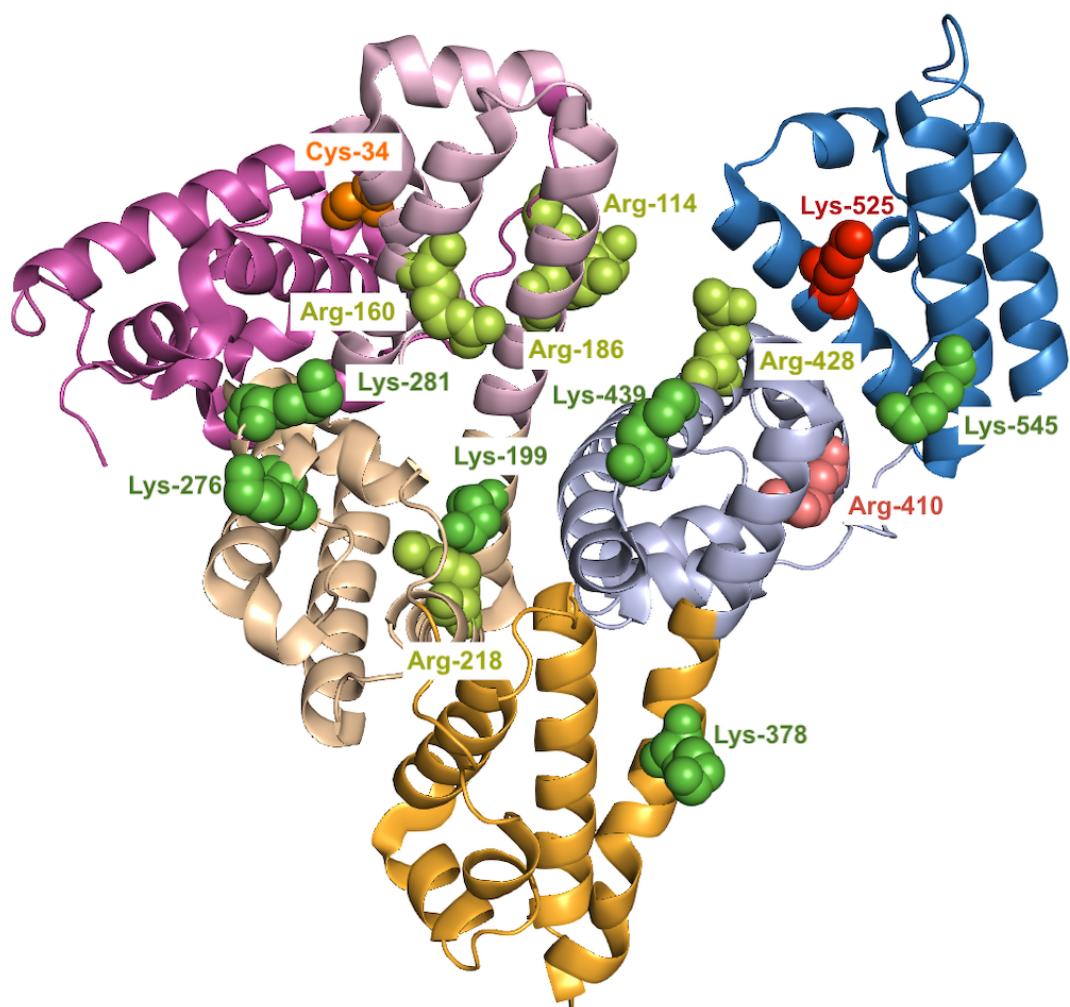
Figure 12. Glycation sites of Human Serum Albumin: the main sites, Lys-525 and Arg-410 (red and light red, respectively), the sites that have lower participation, Lys-199, 276, 281, 378, 439, 545 and Arg-114, 160, 186, 218, 428 (green and green light, respectively), and a possible site of glycation, Cys-34 (orange).

1.4. INTERACTIONS BETWEEN ANTIRETROVIRALS AND ALBUMINS

There are few reported studies about the interaction between antiretrovirals and albumins. The reported studies focus mainly on interaction with BSA, due to its high similarity with HSA, and lower cost compared to the human. Until our knowledge, we did not find any biophysical characterization of the binding between antiretrovirals and g-HSA. For this reason, it was described below only four examples of the target interaction for direct comparison with the data obtained in this project.

The first case was reported by Alanazi, A. M. et al [68], that biophysically studied three FDA-approved antiretrovirals used to inhibit HIV replication (abacavir, efavirenz, and emtricitabine) and BSA. To this study it was used spectroscopic methods (static fluorescence, synchronous fluorescence, three-dimensional fluorescence, and UV-vis absorption) and molecular docking. In the spectroscopic methods the authors used a fixed concentration of BSA (1.5 μM) and used FCT concentration varying from 3.2 until 30 μM. For the spectroscopic measurements, the authors excited albumin at 285 nm. Other specificities on the methods conditions can be found in the description of the article. The conclusions of Alanazi job are that the mechanism of interaction between the BSA and the FCT is static, the K_{sv} (Stern-Vomer constant, obtained using the **Equation 1**) decreased with the temperature (**Table 1**) and the K_q (quenching constant, obtained using the **Equation 1**) are higher than the k_{diff} (difussion rate constant for the water, $10^9 \, M^{-1}s^{-1}$). In this article, to calculate the binding constant, (K) and the number of binding sites (*n*) the authors used the double logarithmic equation (**Equation 2**), and finally, they used the K values to determine the thermodynamic parameters using the **Equation 3** and **Equation 4** (**Table 1**). Basically, they obtained ΔH° < 0 and a ΔS° > 0, so, the interaction between the BSA and the FCT is through electrostatic forces. The negative values for ΔG° indicate that the interaction is spontaneous. With the static fluorescence at 298K also was determined the site of interaction, in this study used two site markers, warfarin (WAR) and ibuprofen (IBUP) that interact specifically into Sudlow's sites I and II, respectively. To determine the binding site were compared the K_{sv} values in absence and presence of markers (**Table 2**), if it is produced a decrease in the K_{sv} value it means that the interaction occur in this site. The results indicate that the interaction can occur in the sites I or site II. To finish, with the molecular docking this statement was confirmed.

$$\frac{F_0}{F} = 1 + k_q \tau_0 [Q] = 1 + K_{SV}[Q] \qquad (1)$$

$$\log\left(\frac{F_0 - F}{F}\right) = \log K + n\,\log[Q] \qquad (2)$$

$$\ln K_{SV} = -\frac{\Delta H°}{RT} + \frac{\Delta S°}{R} \qquad (3)$$

$$\Delta G° = \Delta H° - T\Delta S° \qquad (4)$$

In the **Equation 1**, F_0 and F are the steady-state intensity fluorescence of HSA/BSA/g-HSA in absence and presence of antiretrovirals. The [Q], k_{SV} and K_q are the antiretroviral concentration, Stern-Volmer quenching constant, and bimolecular quenching rate constant, respectively. τ_0 is fluorescence lifetime for HSA without antiretroviral. In the **Equation 2** the K_b and n are the binding constant and the number of binding sites, respectively. In the **Equation 3** and **Equation 4** $\Delta H°$, $\Delta S°$ and $\Delta G°$ are the enthalpy, entropy, and Gibbs free energy change, respectively. T and R are temperature (289, 296, 303 and 310 K) and gas constant (8.3145 J mol^{-1} K^{-1}). with Origin.

Table 1. BSA-FCT constants: K_{sv}, Stern-Volmer constant; k_q, quenching constant; K, binding constant; n, number of binding sites, and thermodynamic parameters [68].

T^a (K)	K_{sv} ($\times 10^4$Lmol^{-1})	k_q ($\times 10^{13}$Lmol^{-1}s^{-1})	K ($\times 10^4$Lmol^{-1})	n	r^2	$\Delta G°$ kJmol^{-1}	$\Delta S°$ Jmol^{-1}K^{-1}	$\Delta H°$ kJmol^{-1}
288	2.06$\pm$0.10	7.62	1.89$\pm$0.2	0.99	0.9970	-23.59		
298	2.04$\pm$0.04	7.56	1.82$\pm$0.2	0.98	0.9993	-24.31	71.88	-2.89
209	2.03$\pm$0.03	7.53	1.75$\pm$0.3	0.98	0.9994	-25.09		

Table 2. BSA-FCT Stern-Volmer constants in the absence and presence of the site markers [68].

	K_{sv} ($\times 10^4$Lmol^{-1})
Only drug	2.04$\pm$0.04
Drug-WAR	0.86$\pm$0.09
Drug-IBUP	1.03$\pm$0.14

Another case is the Shi, J. M. et al. article [69], they studied the interaction between a HIV antiretroviral, darunavir (DRV) and BSA. They used different

spectroscopic methods to their study, like in the first case, only are described the same spectroscopic methods that are used in this project: fluorescence, absorption, and molecular docking. In the fluorescence measurements they used a fixed BSA concentration (1.5 μM) and varying the DRV concentration from 0 until 1.2 μM, exciting the albumin solution at 285nm. In the case of the UV-Vis absorption the BSA concentration was fixed at 0.5μM and the DRV varied from 0 until 60 μM. The rest of spectroscopic conditions are described in the article. The fluorescence results based on K_{SV} and K_q parameters (**Table 3,** obtained using the **Equation 1**) indicate that the mechanism of interaction between BSA and DRV is static: K_{SV} decreased with the increase of temperature and the $K_q > K_{diff}$. In this case, the authors used the absorption to calculate the binding constant, K_b, through the Benesi-Hildebrand equation **(5)**

$$\frac{F_0}{F} = 1 + k_q\tau_0[Q] = 1 + K_{SV}[Q] \qquad (1)$$

$$\frac{1}{A-A_0} = \frac{1}{A-A_0} + \frac{1}{(A_1-A_0)K_b[C]} \qquad (5)$$

in which A_0, A, and A_1 are the absorbance intensities in absence of, at intermediate and infinite concentration of DRV respectively. K_b is the binding constant and C is the DRV concentration. The K_b values (Table 3) decreased with the temperature, so, the stability of the BSA:DRV complex weakened when the temperature rose. With the K_b value the thermodynamic parameters are calculated using **Equation 3** and **Equation 4**, and like ΔH° and ΔS° are negative it deduces that the principles interaction forces are Van der Walls and/or Hydrogen forces; the ΔG° is negative so the interaction between BSA.DRV is spontaneous. To determine the interaction sites, they used phenylbutazone and ibuprofen, that correspond at Sudlow sites I and II respectively and they compared the K_b values in the absence and presence of the markers (**Table 4**). It´s observed a major decreased in the ibuprofen presence thar in the phenylbutazone presence, so, the interaction between the BSA and the DRV is produced in the site II. With molecular docking, they confirmed these results.

$$lnK_{SV} = -\frac{\Delta H°}{RT} + \frac{\Delta S°}{R} \qquad (3)$$

$$\Delta G° = \Delta H° - T\Delta S° \qquad (4)$$

Table 3. BSA-DAR constants: K_{sv}, Stern Volmer constant; k_q, quenching constant; K, binding constant; n, number of binding sites and thermodynamic parameters [69].

T^a (K)	K_{sv} ($\times 10^4$Lmol^{-1})	k_q ($\times 10^{12}$Lmol^{-1}s^{-1})	K_b (Lmol^{-1})	r^2	$\Delta G°$ kJmol^{-1}	$\Delta S°$ Jmol^{-1}K^{-1}	$\Delta H°$ kJmol^{-1}
298	4.42	7.37	1.26×10^4	0.9939	-23.23		
305	4.08	6.80	3.01×10^3	0.9826	-20.73	-357.34	-129.72
310	3.35	5.58	1.71×10^3	0.9974	-18.4		

Table 4. BSA-DRV binding constants in the absence and presence of the site markers [69].

	K_b (Lmol^{-1})
BSA-DRV	1.26×10^4
BSA-DRV-Phenylbutazone	1.24×10^4
BSA-DRV-Ibuprofen	8.18×10^3

The third study case is the Patin, S. et al article [70], in this case they compared the interaction between a HIV-1 reverse transcriptase inhibitor, 4-(4′-cyanophenoxy)-2-(4″-cyanophenyl)-aminoquinoline, and two albumins (BSA and HSA). For this study were used the spectroscopic methods, UV-VIS absorption and fluorescence quenching, and the molecular docking. In the UV-VIS absorption they fixed the BSA and HSA concentration (5μM) and varied the antiretroviral concentration (10-50μM). The BSA/HSA UV-VIS spectrum presented a strong band at 280 nm that it is exhibited slight blue shifts from 280 to 278 nm after the antiretroviral addition, indicating an interaction between the proteins and the antiretroviral. In the fluorescence quenching the BSA/HSA concentration is the same than in the UV-VIS absorption but the antiretroviral concentration is different (2-12μM). In this job they used an equation to correct the internal filter effects (that is described in the next point, **2. Materials and methods)** to recalculate the fluorescence intensities and then, calculate the K_{sv} and k_q constants using the **Equation 1** (**Table 5**). The K_{sv} values decreased with the temperature and $k_q > k_{diff}$, so the interaction mechanism is static. The double logarithmic equation, **Equation 2**, (was used to calculate K_b and n (**Table 5**), and the thermodynamic parameters (**Table 5**) were calculated from the K_b values,

using the **Equation 3** and **Equation 4**. $\Delta H°$ and $\Delta S°$ are negative, so the principles interaction forces are Van der Walls and/or Hydrogen forces; the $\Delta G°$ is negative so the interaction between BSA/HSA and the antiretroviral is spontaneous. In this study the authors employed the double logarithmic equation (log K_b values, **Table 6**) to determine the interaction site, like log K_b in presence of Warfarin has the minor value (to BSA and HSA) the interaction site of this antiretroviral with the albumins is site I and with molecular docking these results were confirmed.

$$\frac{F_0}{F} = 1 + k_q \tau_0 [Q] = 1 + K_{SV}[Q] \qquad (1)$$

$$\log\left(\frac{F_0 - F}{F}\right) = \log K + n \log[Q] \qquad (2)$$

$$ln K_b = -\frac{\Delta H°}{RT} + \frac{\Delta S°}{R} \qquad (3)$$

$$\Delta G° = \Delta H° - T\Delta S° \qquad (4)$$

Table 5. BSA/HSA-4-(4′-cyanophenoxy)-2-(4″-cyanophenyl)-aminoquinoline

	T^a (K)	K_{sv} (x10^4Lmol^{-1})	k_q (x10^{12}Lmol^{-1}s^{-1})	K_b (Lmol^{-1})	n	r^2	$\Delta G°$ kJmol^{-1}	$\Delta S°$ Jmol^{-1}K^{-1}	$\Delta H°$ kJmol^{-1}
BSA	298	3.75	6.25	1.32×10^5	1.13	0.966	-31.25	-73.31	-56.5
	308	3.43	5.71	6.45×10^4	1.08	0.97	-30.86		
	318	3.06	5.10	3.82×10^4	1.05	0.998	-30.36		
HSA	298	2.91	5.19	1.13×10^5	1.14	0.966	-31.09	-58.64	-49.35
	308	2.52	4.50	6.87×10^4	1.09	0.998	-30.75		
	328	2.28	4.07	4.10×10^4	1.06	0.97	-30.05		

constants: K_{sv}, Stern Volmer constant; k_q, quenching constant; K_b, binding constant; n, number of binding sites and thermodynamic parameters [70].

Table 6. BSA/HSA-antiretroviral binding constants in the absence and presence of the site markers [70].

	log K_b (BSA)	log K_b (HSA)
Albumin-Antiretroviral	5.1051	5.0693
Albumin-Antiretroviral-Phenylbutazone	4.4752	4.5315
Albumin-Antiretroviral-Ibuprofen	5.1649	5.0854

The last chosen case study is the Tunç, S. et al job [71] where the authors study the interaction between chloroquine diphosphate (CQP) and phenelzine sulfate (PS) drugs (used in the treatment of various rheumatic diseases, treatment, and prevention of malaria, and has been proposed as a HIV-1 therapeutic agent) and HSA and human hemoglobin, only we will focus on the interaction with the HSA. To this study the authors employed different techniques, those that interest us are fluorescence, UV-VIS, and circular dichroism. To quenching fluorescence, they used a fixed HSA concentration, 50μM, and varied the CQP and PS concentrations, $0-30.0\mu$M and an excitation wavelength at 280nm; to the two compounds was used the equation to correct the internal filter effects and recalculate the intensity fluorescence values. From these values and using the Stern-Volmer equation (**Equation 1**) the authors calculated the K_{SV} and K_q (**Table 7**) to determine the quenching mechanism. Like the K_{SV} value decrease with the temperature and $k_q > k_{diff}$ the mechanism of HSA-CQP interaction is static (in the system HSA-PQ was not observed quenching fluorescence). With the double logarithmic equation (**Equation 2**) K_b and n values was obtained (**Table 7**). The k_b values decrease with the temperature increase, the stability of complex decrease with the temperature. With the k_b values was calculated the thermodynamic parameters using the **Equation 3** and **Equation 4** (**Table 7**) obtaining negative values of $\Delta H°$ and $\Delta G°$ and a positive value of $\Delta S°$, so the main binding force is electrostatic, this interaction was exothermic and spontaneous. To the UV-VIS absorption the authors used the same concentrations like in the quenching fluorescence, in the HSA-CQP UV-VIS spectra was observed a decrease in the HSA absorption with the CQP addition, it means that exists a complex formation. To circular dichroism the HSA concentration was fixed at 5.0μM and the CQP concentration was 5.0 and 30.0μM (HSA-CQP range ratio 1:1 and 1:6), observing

a decrease in HSA α-helices percentage with the increased of CQP concentration, concluding that the HSA structure is modified with the addition of CQP.

$$\frac{F_0}{F} = 1 + k_q \tau_0 [Q] = 1 + K_{SV}[Q] \qquad (1)$$

$$\log\left(\frac{F_0 - F}{F}\right) = \log K + n \log[Q] \qquad (2)$$

$$lnK_b = -\frac{\Delta H°}{RT} + \frac{\Delta S°}{R} \qquad (3)$$

$$\Delta G° = \Delta H° - T\Delta S° \qquad (4)$$

Table 7. HSA-CQP constants: K_{sv}, Stern Volmer constant; k_q, quenching constant; k_b, binding constant; n, number of binding sites and thermodynamic parameters [71]

T^a (K)	K_{sv} ($\times 10^4$ Lmol^{-1})	k_q ($\times 10^{12}$ Lmol^{-1}s^{-1})	k_b (Lmol^{-1})	n	r^2	$\Delta G°$ kJmol^{-1}	$\Delta S°$ Jmol^{-1}K^{-1}	$\Delta H°$ kJmol^{-1}
288.15	1.83	1.83	2.65×10^4	1.04	0.8992	-24.44		
298.15	1.66	1.66	2.25×10^4	1.03	0.9953	-24.79	34.62	-14.47
310.15	1.57	1.57	1.81×10^4	1.01	0.9960	-25.21		
318.15	1.49	1.49	1.48×10^4	1.00	0.9881	-25.48		

In this project we recur at the more popular techniques used in the studies of protein-antiretrovirals interactions: UV-VIS absorption, quenching fluorescence, and molecular docking, using these four articles to compare the methodology and the results, and we will complement the information with time-resolved fluorescence and isothermal titration calorimetry.

1.5. OBJECTIVES

The objective of this project is studying the interaction between serum albumin (human serum albumin, bovine serum albumin and human serum albumin glycated) and the antiretrovirals. This information let us know, or deduce, how the drugs are transported in the organism; and, in the case they are transported by the albumin, we can know in which albumin site they interact. In the first group of antiretrovirals, family of tenofovir (TFV, TDF, and TAF), exist different properties between the three antiretrovirals (relatively to the bioavailability and stability); for this reason, it's an interesting factor to study the interaction between this antiretrovirals and the albumin, to know if the affinity of this drugs and the protein and the binding site it´s different too.

The other objective of this project is, before study the interaction between the two albumin and the six antiretrovirals, focus in two antiretrovirals (one of the family of tenofovir and the other of the second group) and determine its interaction with the glycated albumin. There aren´t many studies about the interaction between the antiretrovirals and the glycated albumin (presented in diabetic persons) and its know that the presence of glycose molecules in the HSA modify its functional properties (protein activity, folding, degradation, and cell function). For this reason, the second part of this project is focalized in the study of the interaction between some antiretrovirals and the glycated albumins, to know if the effect of glycation affects positively, negatively or no-affect to the bind between the protein and the drugs.

CHAPTER 2:
MATERIALS AND METHODS

2.1. Stock solutions

All chemical reagents are provided from Sigma-aldrich, with some particularity. HSA (catalog number: A3782) is lyophilized powder, and fatty acid and globulin free; with a purity ≥99%. BSA (catalog number: A7030) is a heat shock fraction, and protease, fatty acid and essentially globulin free; with a purity ≥98% in pH 7. g-HSA (catalog number: A8301) is lyophilized powder. All albumins stock solutions are 10 μM and there are prepared in PBS (phosphate buffered saline).

TFV (catalog number: SML1795) has a purity of ≥98%. TDF (catalog number: PMR1957) is a pharmaceutical secondary standard and a certified reference material, with a purity ≥96%. TAF (catalog number:). FCT (catalog number: SML3051) has a purity ≥98%. 3TC (catalog number: L1295) has a purity ≥98%. AZT (catalog number: PHR1292) is a pharmaceutical secondary standard and a certified reference material. All antiretrovirals solutions are 1 mM and there are prepared in deionized water.

The PBS solution is prepared to a final volume of 500 ml and has the next composition: 137mM NaCl, 2.7mM KCl, 8mM Na_2HPO_4, 2mM KH_2PO4; and its pH is near to 7.4.

2.2. Molecular Docking (MD)

The chemical HSA structure was obtained in the protein Data Bank (PDB), which the next access codes: 1E7A, 1E7B; 1E7C, 1E7F, 1E7H, 1gni, 1N5U, 2BXA, 2BXH, 2BXK, 2BXP, 2VUE, 2XW0, 4E99, 4L8U, 4L9K, 4L9O, 6EZQ, 6HSC, 6WUW. The ligands structures (TFV, TADF, TAF, FCT, 3TC, and AZT) were built and energy-minimized with Spartan´14 software [72] by Density Functional Theory (DFT) method. The molecular docking calculations were made with Gold 2.0 software (CCDC, Cambridge Crystallographic Data Center) [73]. The molecular docking calculation are made with a 10Å radius around the selected amino acid residue present in each one of the interaction sites: Trp-213, Tyr-161, and Tyr-411 residues to sites I, II and III respectively. It was used the score function 'ChemScore' due to the lowest room mean square deviation (RMSD) value obtained by redocking studies. The figures are generated by PyMol Molecular Graphics System 1.0 level software (Delano Scientific LLC Software) [74].

2.3. UV-Vis absorption

Agilent Cary 5000-UV-Vis-NIR spectrometer is used to register de absorption spectra of compounds at room temperature. Three different spectra are measurement in a quartz cell with 1.0 cm optical path in the 200-800 nm range

with a PBS as line base: HSA spectra of the HSA stock solution (10 μM); antiretrovirals spectra (8 – 26 μM, stock solutions diluted in PBS) and HSA:antiretrovirals spectra (with a fixed HSA concentration, 10 μM, and a antiretrovirals concentration with a same range previously described).

2.4.   Steady-state fluorescence (SSF)

For steady-state fluorescence measurements is used the Horiba-Jobin Yvon Fluorolog 3.2.3 coupled with thermostat cuvette holder. The measurements are made in the 320-350 range at four different temperatures (289, 296, 303, and 310 K) with a λ exc = 295 nm. The spectra obtained with this technique are made in the same conditions that absorption spectra: only HSA/BSA/g-HSA (10 μM) and albumin:antireroviral (with the fixed HSA/BSA/g-HSA concentration and the same range of antiretrovirals used in absorption).

In some cases, is necessary a filter correction in the fluorescence intensity values, this occurs when the antiretrovirals present absorption in the HSA excitation and maximum absorption (295 and 338 nm, respectively) and the steady-state fluorescence data are corrected in terms of the inner filter effect, according to the (**Equation 6**) [75, 76]:

$$F_{cor} = F_{obs}\ 10^{[\frac{A_{ex}+A_{em}}{2}]} \tag{6}$$

in which F_{cor} and F_{obs} are corrected and observed steady-state fluorescence, respectively; A_{ex} and A_{em} are the absorption value at the excitation (295 nm) and maximum fluorescence emission (338nm), respectively.

To obtain quantitative parameters on the binding affinity HSA/BSA/gHSA and antiretrovirals, Stern-Volmer (**Equation 1**), double-logarithmic (**Equation 2**), van´t Hoff (**Equation 3**) and Gibbs´free energy (**Equation 4**) were applied [76-78].

$$\frac{F_0}{F} = 1 + k_q \tau_0 [Q] = 1 + K_{SV} \tag{1}$$

$$\log\left(\frac{F_0-F}{F}\right) = logK_b + n\ log[Q] \tag{2}$$

$$lnK_{SV} = -\frac{\Delta H°}{RT} + \frac{\Delta S°}{R} \tag{3}$$

$$\Delta G° = \Delta H° - T\Delta S° \tag{4}$$

in which F_0 and F are the steady-state intensity fluorescence of HSA/BSA/g-HSA in absence and presence of antiretrovirals. The [Q], antiretroviral concentration; K_{SV}, Stern-Volmer extinction constant that is considered an association constant

for the following reasons (that are confirmed in the following points of this work): the mechanisms in the interactions studied are static (there is an association in the ground state between the fluorophore and the inhibitor, and the complex has no residual fluorescence) and the protein has only one binding site; and k_q, bimolecular quenching rate constant [76, 79, 80] . τ_0 is the obtained experimental average fluorescence lifetime for HSA without antiretroviral in PBS (around $\tau_0 = 6$ ns in this work). The K_b and n are the binding constant and the number of binding sites, respectively. $\Delta H°$, $\Delta S°$ and $\Delta G°$ are the enthalpy, entropy, and Gibbs free energy change, respectively. T and R are temperature (289, 296, 303 and 310 K) and gas constant (8.3145 J mol^{-1} K^{-1}). For each antiretroviral concentration, triplicate experiments were performed (to HSA and BSA, in g-HSA was realized only one experiment) and the data were analyzed with Origin.

2.5. Time-resolved fluorescence (TRF)

Time-resolved fluorescence (TRF) decays were obtained through a home-built-time-correlated single photon counting (TCSPC) apparatus previously described [81]. The decays were collected with excitation at 282 nm (HoribaJobin-Yvon-IBH nanoLED) and emission wavelength at 338 nm. The fluorescence decays for HSA (10 μM, in PBS) and HSA:TFV/AZT (antiretroviral concentrations of 8.21, 9.84, 19.5 and 25.8 μM in PBS) and HSA:TDF (antiretroviral concentrations of 8.21, 9.84 and 16.3 μM in PBS), as well as the instrumental response function (IRF, collected using a Ludox® dispersion) were obtained using 1024 channels until 2000 counts at the maximum were reached). Deconvolution of the fluorescence decays curves was performed using modulation function method, as implemented by G. Striker in the SAND software, as previously reported in the literature [82].

2.6. Isothermal titration calorimetry (ITC)

Isothermal titration calorimetry (ITC) experiments were performed on a Malvern, MicroCal VP-Isothermal Titration Calorimetry at 289K, with injection speed 0.5 μL/s, stirring speed 459 rpm, and reference power 10 μcal/s. The titration was performed with additions of 10 μL/step. The HSA concentration was 239 μM for HSA that was introduced in the cell and the TFV/TDF/TAF concentrations were 2390 μM introduced in the syringe. The other three antiretrovirals, FCT/3TC/AZT had a concentration of 1384 μM and the HSA in theses case had a concentration of 138,4 μM. For the g-HSA experiment was used a concentration of 114,3 μM to g-HSA and of 1143 μM to the AZT. All solutions were previously degassed for 5 min. The obtained thermograms were integrated using data analysis software Origin 7.0 as modified by Microcal to deal with ITC

experiments [83] obtaining de K_{sv} and n values, and the thermodynamic parameters.

CHAPTER 3:
RESULTS AND DISCUSSION

3.1.   Identification of HSA binding site with molecular docking

Sudlow and co-workers defined two principal HSA binding sites located in hydrophobic regions: Site I (warfarin or phenylbutazone binding site, located in the subdomain IIA) and site II (ibuprofen binding site, located in the subdomain IIIA) [84]. Posteriorly it was described a third binding site, site III (digitoxin binding site, located in subdomain IB) [85, 86]. To have a main idea of the main HSA binding site with the antiretrovirals, molecular docking study with 20 HSA structures (PDB bank) and the 6 antiretrovirals was done.

The first step was the calculation of the root-mean-square deviation of atomic positions, or simply root-mean-square deviation (RMSD) using Pymol, that is used as a quantitative measure to compare the similarity between two protein structures, in this case the two PDB Bank molecules with the minor resolution (1.9 Å), 1N5U and 6HSC, were used like mother molecules to compare with the other molecules. The results of this first step are represented in **Table 2** and **Table 3** in the **Appendix.** The results indicate that the minor RMSD value was obtained with the function Super RMSD to the two mother molecules. This function was selected to do the next step in the redocking.

Next step of redocking study was made to select the function that was to be used in the docking study using Golden 2.0 program. The first thing in this step was the elimination of water molecules because these molecules can interfere with the ligands and then the hydrogen atoms were added. Then the ligands of the PDB molecules were deleted and then were put again to determine the minor value of the three possible functions: RSMD ChemPLP, ChemScore or ASP. The results are represented in the **Table 4** in the **Appendix**. The function chosen to do the molecular docking is the function that had a minor value, in this case is the ChemScore.

Once the function is chosen, the molecular docking was made. The first step was the elimination of all ligands of the PDB molecules because the ligands can be near to the binding sites, and they do not allow that the antiretrovirals interact with those sites. To the study of the interaction with the site I the residue Trp-213 was selected, with the site II was the Tyr-161 and with the site III was the Tyr-411. In the case of molecular docking study, the best value is the most positive. The results appear represented in the **Table 5** in the **Appendix**; the site III had the most positive values. In the case of zidovudine there is not results because the molecule gave an error.

The docking results indicate that the preference binding site between the HSA and the antiretrovirals is the site III, these results will be completed with a fluorescence analysis.

3.2. UV-Vis absorption analysis

Absorption spectroscopy in UV-Vis is a straightforward method that has been applied frequently to explore structural changes and complex formation between biomacromolecules and small molecules [87, 88]. There are two main mechanisms for the interaction between macromolecules and small molecules: static and dynamic. In static mechanism changes in the absorption spectrum due to a formation of a complex in a ground-state can be observed. On the other hand, there are not changes in the absorption spectrum when the mechanism is dynamic, only the excited state of the fluorophores is affected [88-91]. UV-VIS spectra were obtained from free HSA, antiretroviral, and HSA:antiretroviral to obtain initial information on the HSA:antiretroviral interaction. HSA spectrum has two absorption maximums (**Figure 13**), at 220nm, attributed to n→π* and π→π* transitions which are associated with the carbonyl group of peptide bound and, at 280 nm, attributed to n→π* transition which are associated with the aromatic amino acid residues phenylalanine (Phe), tryptophan (Trp), and tyrosine (Tyr) [76]. In the **Figure 13** is represented the absorption spectra of TFV and 3TC when the proportion [HSA]:[TFV]/[3TC] is 1:1, the absorption spectra of the other antiretrovirals are in the **Figure 1** of the **Appendix**. It can see in the **Figure 13** that the absorption profile of the TFV and 3TC is much lower than the HSA absorption, this is observed to all antiretrovirals except in the FCT spectrum (**Figure 1**, **Appendix**) so, in most cases is not necessary a filter correction in its steady-state fluorescence data, only in the FCT study [75,76].
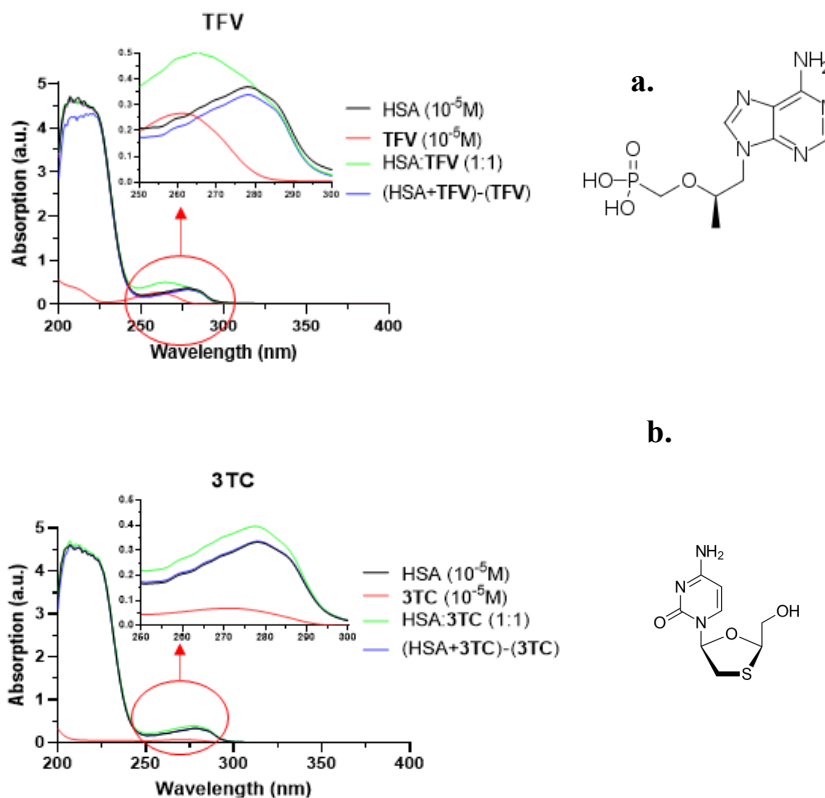
Figure 13. UV-VIS absorption spectra to HSA, HSA:TFV (1:1), and TFV (**a**), and HSA, HSA:3TC (1:1), and 3TC (**b**)

The spectrum of the antiretroviral is subtracted from the absorption spectrum of HSA:antiretrovirals, so is obtained the real spectrum of HSA:antiretrovirals without contribution of antiretrovirals. It is not observed a hyperchromic effect in the HSA spectrum after the addition of the antiretrovirals, this effect would indicate a ground-state association, a static quenching. When changes in the absorption are not observed it usually corresponds at a dynamic quenching, or collisional quenching, because only affects the excited state of the fluorophore [88-91]. In these UV-VIS spectra is not observed any changes after the addition of the antiretroviral, so, initially, it can suppose that the mechanism of interaction is dynamic but exists the possibility that the interaction be weak and for this reason there are no altercations in the spectra. These data will be confirmed with another techniques.

3.3. Steady-state fluorescence analysis

Steady-state fluorescence is the method more used to study the interaction between two compounds; with this method it is intended to expand the information obtained with the UV-VIS analysis. In this analysis were used two different serum albumins: Human and Bovine, because the HSA only has a Trp fluorophore, Trp-214 (near to the site I), however, the BSA has two fluorophores, Trp-212 and Trp-134 (near to the site I and III, respectively) [60]. The molecular docking results obtained indicate that the preferred site of the serum albumin from the antiretrovirals is the site III, which is only "marked" with a Trp in the BSA, so, for this reason are used the two albumins, to compare the quenching data between the two albumins and see if exists any difference.

Usually, the fluorescence experiments are done at a λ_{exc}= 280 nm, wavelength at which Trp, Tyr and Phe amino acids are excited, Phe has a quantum yield very low (does not absorb significantly at this wavelength). Tyr fluorescence is totally quenched if it is ionized or near a carbonyl group, amino acid, or a Trp. So, the higher absorptivity coefficient and fluorescence quantum yield of Trp, and the Tyr efficient fluorescence resonance energy transfer to Trp are the factors that confirm that the only emission observe is from Trp (at 340nm) [70, 91].

However, in this project the λ_{exc}= 295 nm was preferred because the most antiretrovirals do not present absorption at this wavelength (so, it is not necessary a filter correction, only for the FCT study). Experiments were performed at λ_{exc}= 280 and 295 nm with HSA and BSA (**Figure 14**) in order to check the equivalence of those wavelength of excitation in respect to quenching studies with (anti-retroviral) drugs. In **Figure 14a** is represented the fluorescence quenching when the λ_{exc}= 295 nm with BSA and HSA. It was observed that the fluorescence intensity of BSA is higher than fluorescence intensity of HSA because at 295 nm the intrinsic fluorescence is exclusively produced by the Trp residue (the BSA has two Trp residue however the HSA only has one). When the λ_{exc}= 280 nm (**Figure 14b**) it is observed that the fluorescence intensity is higher than with excitation at λ_{exc}= 295 nm this phenomenon is due to the fact that the solution absorptivity at 280nm is higher. One important observation from these experiments is that the percentage of quenching of the protein fluorescence in presence of TFV is identical with both protein (BSA and HAS) when excited at the same wavelength and this percentage is lower when excited at 295 nm than excited at 280 nm (for both proteins, **Figure 14**). It can be seen in the **Figure 15** that the absorption to HSA and BSA at 280 and 295 nm are very similar; with values of 3.63×10^{-1} and 8.21×10^{-2}, for HSA at 280 and 295 nm respectively and 4.3×10^{-1} and 8.64×10^{-2}, for BSA at 280 and 295 nm respectively.
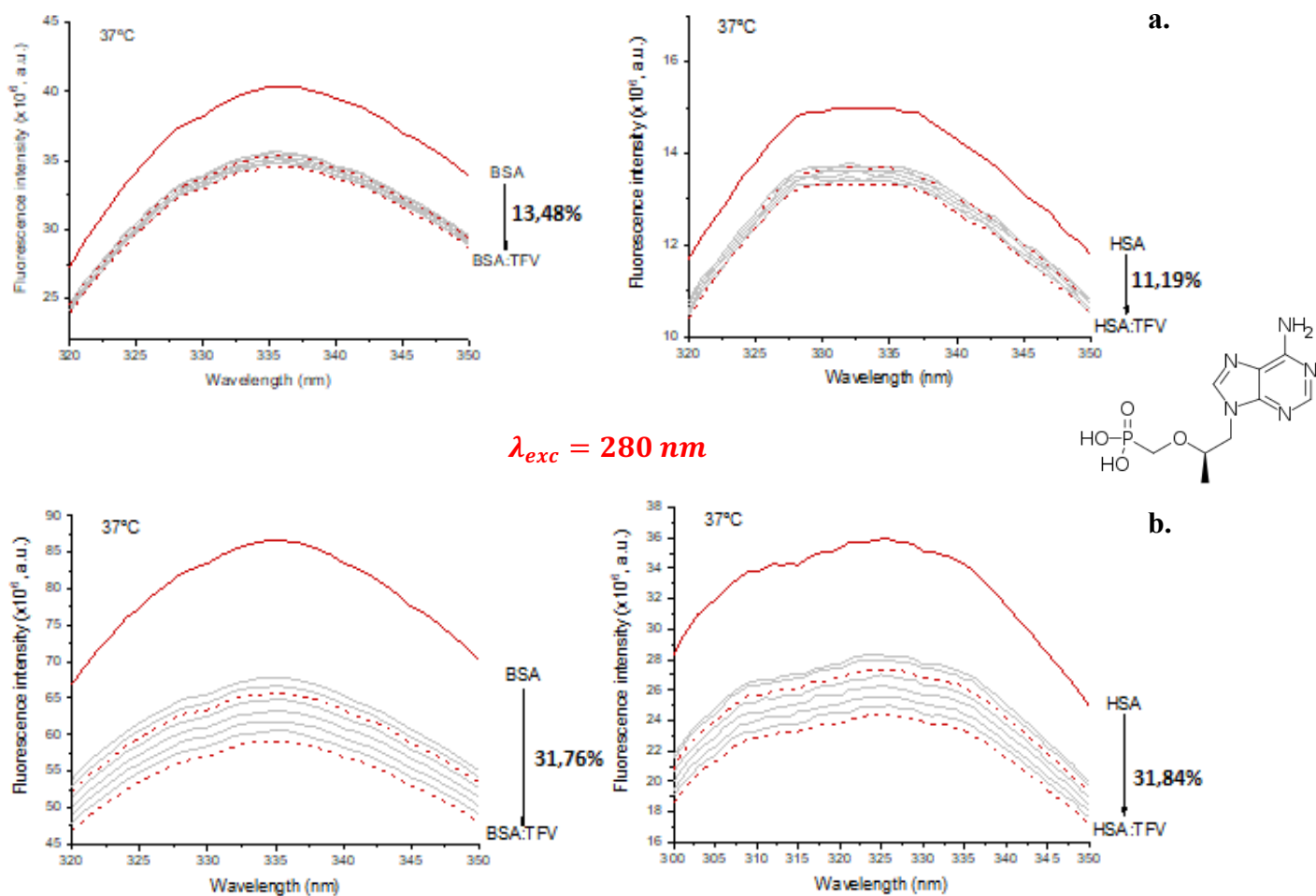
$$\lambda_{exc} = 295\ nm$$

$$\lambda_{exc} = 280\ nm$$

Figure 14. Quenching fluorescence of BSA/HSA-TFV when λ_{exc}= 295 nm (**a**) and when λ_{exc}= 280 nm (**b**) at [TFV]= $8 - 26\ \mu$M. Red line is the emission of protein. The fist red dotted line corresponds at the proportion 1:1 between the HSA:antiretroviral. The last red dotted line corresponds at the maximum concentration of the antiretrovirals.
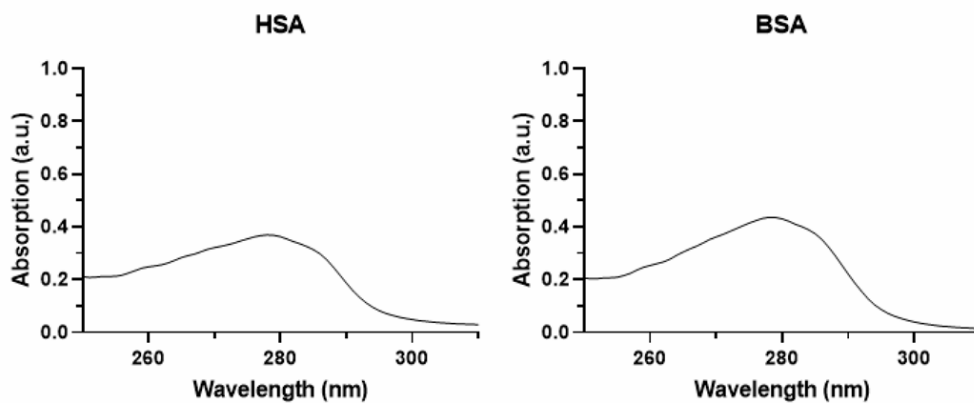

Figure 15. UV-VIS absorption spectra to HSA and BSA. Absorption HSA at 280 and 295 nm are 3.63×10^{-1} and 8.21×10^{-2}, respectively. Absorption BSA at 280 and 295 nm are 4.30×10^{-1} and 8.64×10^{-2}, respectively.

Once the excitation wavelength was chosen, at 295nm, the experiments were realized for all the antiretrovirals to evaluate the binding capacity between the antiretrovirals and the two albumins (HSA and BSA), and the type of interaction mechanism between the two molecules: static or dynamic quenching. For the two mechanism the fluorophore and the quencher must be in contact. The collisional or dynamic quenching occur when the quencher diffuses to the fluorophore during the lifetime of the excited state; upon contact, the fluorophore returns to the ground state without emission. However, in the static quenching occur a bind between the fluorophore and the quencher forming a non-fluorescent complex in the ground state [76].

With the quenching fluorescence the Stern-Volmer and Van Toff representations for HSA/BSA-TFV and HSA/BSA-FCT can be obtained (**Figure 16**); the other Stern-Volmer and Van Toff plots are represented in the **Figure 2** of **Appendix**. A linear Stern-Volmer plot indicates that only exists a single class of fluorophores [72], all equally accessible to quencher, and only one type of quenching occurs, but this plot does not prove that collisional or static quenching have occurred. The two mechanisms can be distinguished by their differing dependence on temperature (for this reason the steady state fluorescence was realized at four temperatures), or preferably by lifetime measurements (time resolved fluorescence). Higher temperatures result in faster diffusion and hence larger amounts of collisional quenching, typically result in the dissociation of weakly bound complexes (smaller amounts of static quenching) [76]. In the **Figure 16** it can see four linear Stern-Volmer plots with λ_{exc} of 295nm, it means that only exists a type of fluorophore accessible to quencher, the tryptophan residue (in the case of HSA only one Trp, and in the case of BSA two Trp residues).
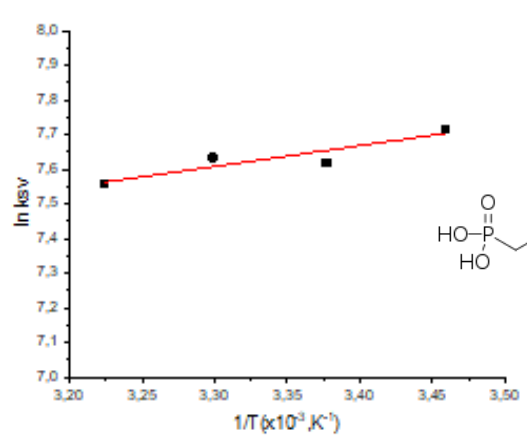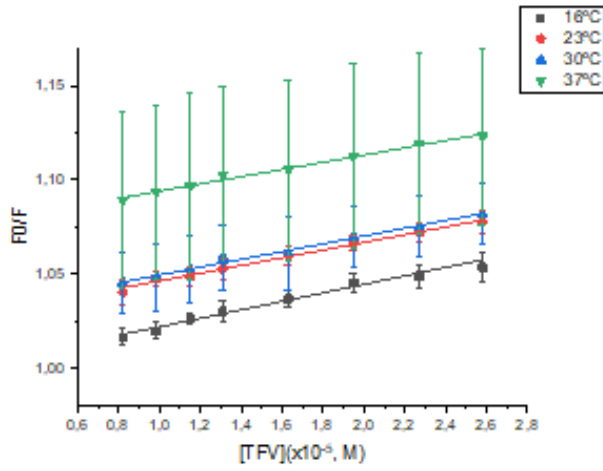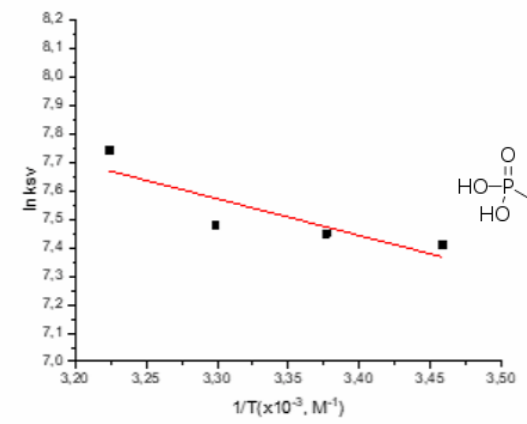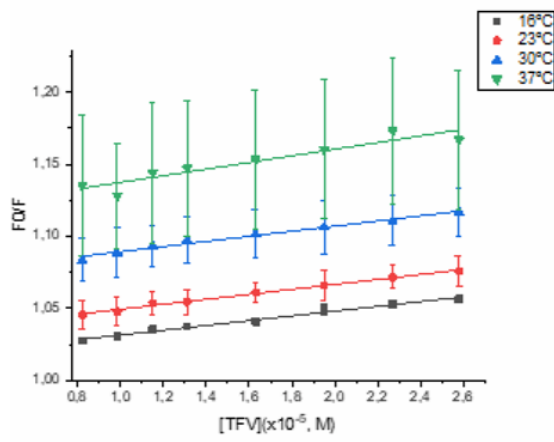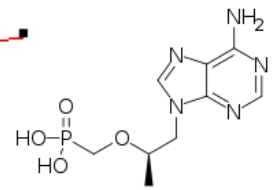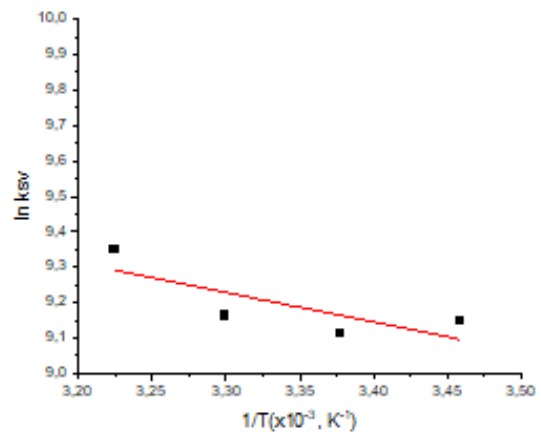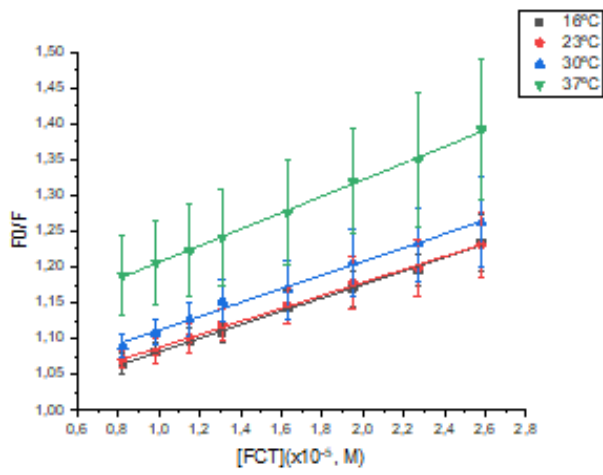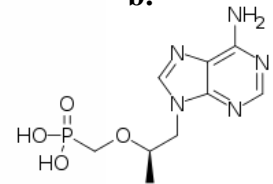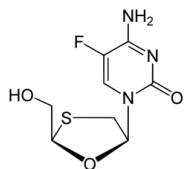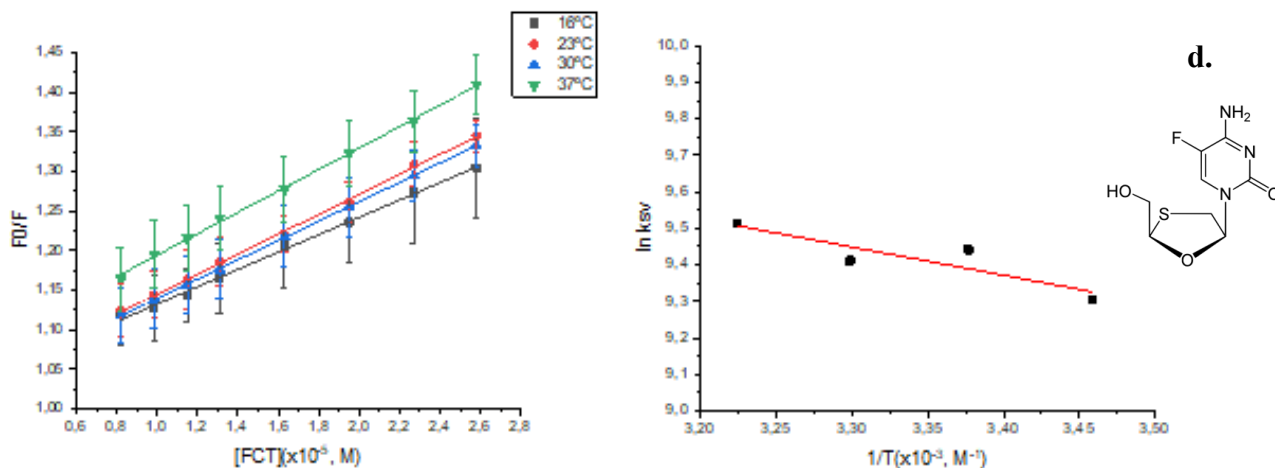
Figure 16. Stern-Volmer and Van Toff representations of HSA-TFV (**a**), BSA-TFV (**b**), HSA-FCT (**c**) and BSA-FCT (**d**) at λ_{exc}= 295nm.

      With the Stern-Volmer plots the K_{sv} constant can be calculated, and the Van Toff plots can be made, and the thermodynamic parameters can be obtained (**Eq. 2 and Eq. 4**) With the double logarithmic equation (**Eq. 3**) the n value is calculated. All the values are represented in the **Table 8** to HSA and **Table 9** to BSA. It is not observed an obviously tendency in the K_{sv} values, so it is not possible identified the quenching mechanism only with the K_{sv} values; it is necessary to do another experiment, time-resolved fluorescence, to calculate the k_q and determine the type of quenching. The n values are near to 1, so the stoichiometry is 1:1. The thermodynamic parameters indicate that most interactions are endothermic, absorb heat ($\Delta H>0$), except the HSA-TDF, HSA-TFV and BSA-3TC interactions that are exothermic, release heat ($\Delta H<0$). All the processes have a $\Delta S>0$, that means that the reactions are entropically directed favoring a $\Delta G>0$, that is, spontaneous reactions. These values can be confirmed with more precise techniques, like ITC.

Table 8. K_{sv} HSA-antiretrovirals constant, n values and thermodynamic parameters, the error was obtained by performing experiments in triplicate.

Molecule	T^a K	K_{sv} ($\times 10^3$) $Lmol^{-1}$	n	$\Delta H°$ $kJmol^{-1}$	$\Delta S°$ $Jmol^{-1}K^{-1}$	$\Delta G°$ $kJmol^{-1}$
TAF	289,15	2.77±0.10	0.96±0.03	4.8±3.1	0.083±0.010	-28.7
	296,15	3.04±0.11	0.76±0.02			-29.3
	303,15	2.83±0.19	0.43±0.02			-29.9
	310,15	3.30±0.19	0.37±0.02			-30.4
TDF	289,15	2.15±0.12	1.06±0.06	-3.5±1.2	0.052±0.004	-18.4
	296,15	2.05±0.07	0.56±0.02			-18.8
	303,15	2.07±0.09	0.56±0.03			-19.2
	310,15	1.91±0.09	0.33±0.01			-19.5
TFV	289,15	2.25±0.13	0.99±0.07	-5.0±1.6	0.047±0.005	-18.5
	296,15	2.04±0.08	0.54±0.02			-18.8
	303,15	2.07±0.08	0.56±0.04			-19.2
	310,15	1.91±0.09	0.33±0.01			-19.5
FCT	289,15	9.41±0.17	1.11±0.02	6.9±3.9	0.100±0.012	-21.9
	296,15	9.07±0.21	1.04±0.03			-22.5
	303,15	9.57±0.32	0.90±0.03			-23.2
	310,15	11.5±0.18	0.66±0.02			-23.9
3TC	289,15	1.89±0.04	1.45±0.05	16.9±8.5	0.120±0.028	-17.8
	296,15	1.81±0.12	0.78±0.06			-18.7
	303,15	1.99±0.13	0.63±0.04			-19.5
	310,15	3.12±0.11	0.48±0.02			-20.4
AZT	289,15	3.20±0.07	1.39±0.08	2.5±1.5	0.075±0.005	-19.4
	296,15	3.20±0.14	0.66±0.03			-19.9
	303,15	3.19±0.10	0.44±0.02			-20.4
	310,15	3.46±0.15	0.42±0.02			-20.9

Table 9. K_{sv} BSA-antiretrovirals constant, n values and thermodynamic parameters, the error was obtained by performing experiments in triplicate.

Molecule	T^a K	K_{sv} (x10^3) Lmol^{-1}	n	ΔH° kJmol^{-1}	ΔS° Jmol^{-1}K^{-1}	ΔG° kJmol^{-1}
TAF	289,15	2.98±0.16	1.10±0.08	5.5±4.3	0.085±0.014	-19.1
	296,15	2.78±0.15	0.66±0.02			-19.7
	303,15	2.93±0.11	0.45±0.01			-20.3
	310,15	3.50±0.27	0.38±0.01			-20.9
TDF	289,15	1.62±0.07	1.10±0.08	15.5±10.8	0.114±0.036	-17.5
	296,15	1.63±0.04	0.66±0.02			-18.3
	303,15	1.55±0.03	0.45±0.01			-19.1
	310,15	2.70±0.03	0.38±0.01			-19.9
TFV	289,15	1.65±0.08	1.10±0.08	10.7±430	0.098±0.014	-17.7
	296,15	1.72±0.06	0.66±0.02			-18.4
	303,15	1.77±0.10	0.45±0.01			-19.1
	310,15	2.30±0.34	0.38±0.01			-19.8
FCT	289,15	11.0±0.25	1.13±0.03	6.4±2.3	0.100±0.008	-22.4
	296,15	12.6±0.17	1.07±0.01			-23.1
	303,15	12.2±0.07	0.93±0.01			-23.8
	310,15	13.5±0.23	0.81±0.02			-24.5
3TC	289,15	3.19±0.13	1.75±0.20	-7.9±4.6	0.039±0.015	-19.2
	296,15	2.47±0.09	0.60±0.02			-19.5
	303,15	2.52±0.09	0.60±0.03			-19.8
	310,15	2.48±0.13	0.50±0.01			-20.0
AZT	289,15	2.56±0.13	0.86±0.04	1.0±14.2	0.057±0.047	-18.3
	296,15	1.47±0.11	0.52±0.05			-18.8
	303,15	2.21±0.08	0.40±0.02			-19.3
	310,15	2.32±0.07	0.34±0.01			-19.7

The next part of this project is to study the interaction of the same antiretrovirals with the glycated albumin (gly-HSA). For that, the same steady-state fluorescence conditions were used and the Stern-Volmer and Van Toff plots were obtained (**Figure 17**). This experiment was only done with FCT and AZT. It is observed a linear tendence in the Stern-Volmer plot, that indicates that only exists a single class of fluorophores, the Trp residue.
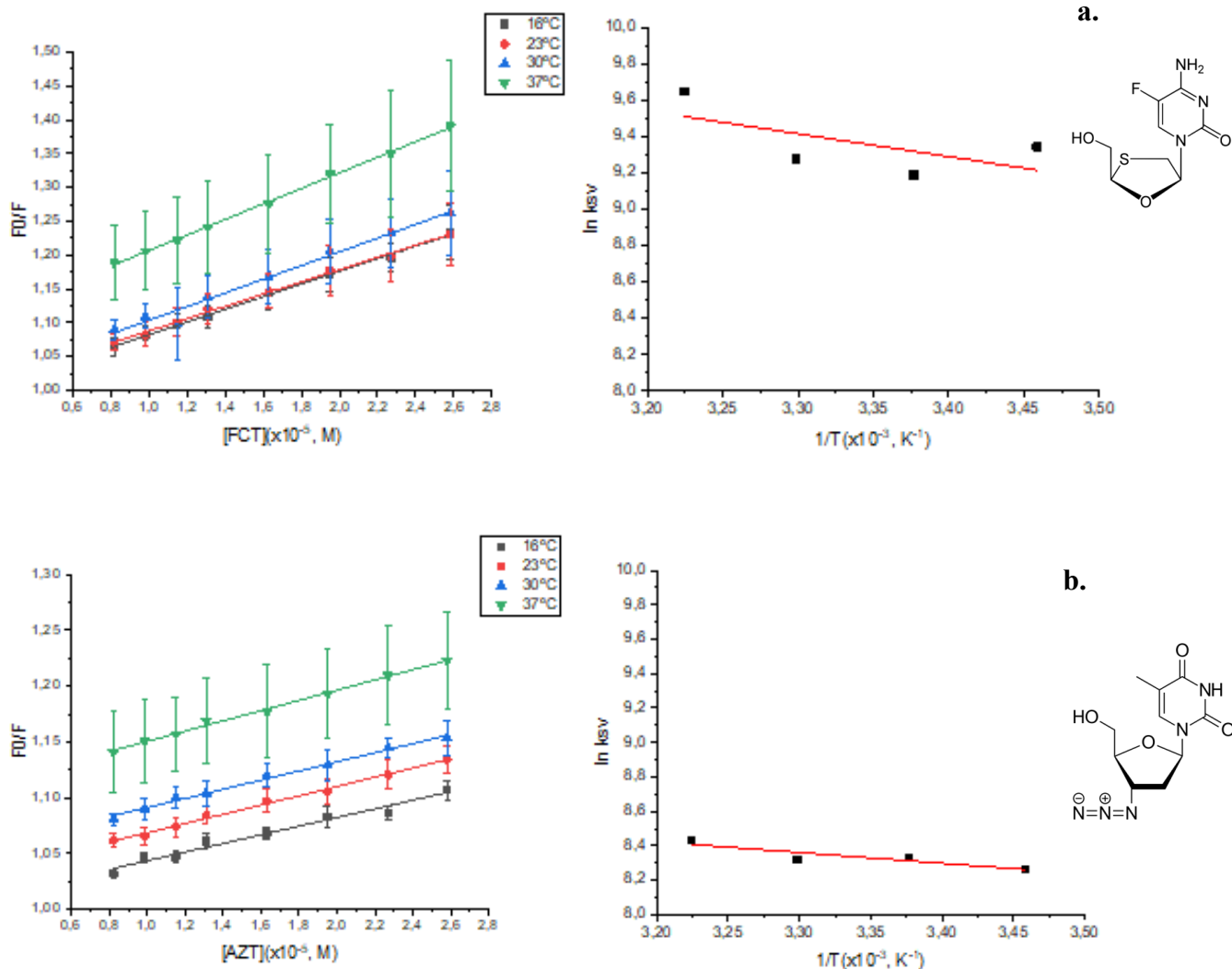
Figure 17. Stern-Volmer and Van Toff representations of gHSA-FCT (**a**) and gHSA-AZT (**b**).

With the Stern-Volmer and Van Toff plots it calculate the constants and thermodynamic parameters represented in **Table 10**. It is not observed a tendency in K_{sv} constants, like in the cases of HSA and BSA. The g-HSA K_{sv} values are higher compared with the HSA and BSA K_{sv} values, it indicates that the interaction between g-HSA and the two antiretrovirals (FCT and AZT) are more favorable that the interaction between those two antiretrovirals and the HSA or BSA. The n values are near to 1, so the stoichiometry is 1:1. The interactions are endothermic ($\Delta H>0$), entropically directed ($\Delta H>0$) and spontaneous ($\Delta G<0$), like in the cases of HSA and BSA. These hypotheses can be confirmed with another technique, ITC.

63

Table 10. K_{sv} gHSA-antiretrovirals constant, n values and thermodynamic parameters.

Molecule	T^a K	K_{sv} (x10³) Lmol⁻¹	n	ΔH° kJmol⁻¹	ΔS° Jmol⁻¹K⁻¹	ΔG° kJmol⁻¹
FCT	289,15	11.4±0.18	1.00±0.02			-22.1
	296,15	9.79±0.30	0.86±0.02	10.5±9.0	0.113±0.030	-22.9
	303,15	10.7±0.14	0.84±0.01			-23.7
	310,15	15.5±0.19	0.84±0.01			-24.5
AZT	289,15	3.88±0.27	0.96±0.07			-19.8
	296,15	4.15±0.12	0.70±0.02	5.2±1.8	0.087±0.006	-20.5
	303,15	4.10±0.15	0.56±0.01			-21.1
	310,15	4.59±0.13	0.41±0.02			-21.7

3.4. Time-resolved fluorescence (TRF) analysis

For moderate quenching concentrations both quenching mechanisms, static and dynamic, presented a linear inclination in the Stern-Volmer plot, so it is not possible to distinguish the two mechanisms only with the steady-state fluorescence study. The measurement of fluorescence lifetimes is the most definitive method to distinguish the static and dynamic quenching, for this reason, is realized a time-resolved fluorescence study with the albumin and three antiretrovirals (TDF, TFV and AZT) [92]. Time-resolved fluorescence is an effective method to determine the quenching mechanism between drugs molecules on biomacromolecules. The fluorescence lifetime decay parameters are obtained by the following equation:

$$\tau = \tau_1 A_1 + \tau_2 A_2 \qquad (7)$$

Where τ_1 and τ_2 are the decay times, A_1 and A_2 are the pre-exponential factors [93]. In other works, it observed that the fluorescence for the Trp in HSA yields three lifetimes [94]. The two first lifetimes are observed for the free-Trp, the third, the longest, results from the interaction between the Trp residue and its microenvironment in the protein matrix. The first lifetime is too short, and it is not observed with the equipment used in this project, existing only two lifetimes in the presented results [95]. For the time-resolved fluorescence the values of the decay times and respective pre-exponential factors are presented in **Table 11**.

Table 11. Decay times, τ_1 and τ_2, pre-exponential factors, A_1 and A_2, and time percent, $\%t_1$ and $\%t_2$ at λ_{exc}=282nm.

Compounds	Proportion HSA:antiretroviral	τ_1 ns	τ_2 ns	A_1	A_2	% t_1	% t_2
TDF	1:0	2,18	6	0,488	0,512	0,26	0,74
	1:0.8	2,41	6,17	0,521	0,479	0,30	0,70
	1:1	2,24	6,05	0,485	0,515	0,26	0,74
	1:1.6	2,15	6,07	0,477	0,523	0,24	0,76
TFV	1:0	2,26	6,16	0,504	0,496	0,27	0,73
	1:0.8	2,26	6,18	0,513	0,487	0,28	0,72
	1:1	2,29	6,3	0,534	0,466	0,29	0,71
	1:1.9	2,36	6,04	0,49	0,51	0,27	0,73
	1:2.6	2,6	6,5	0,573	0,427	0,35	0,65
AZT	1:0	2,12	6,11	0,504	0,496	0,26	0,74
	1:0.8	2,36	6,25	0,543	0,457	0,31	0,69
	1:1	2,04	6,01	0,5	0,5	0,25	0,75
	1:1.9	2,32	6,25	0,518	0,482	0,29	0,71
	1:2.6	2,42	6,31	0,538	0,462	0,31	0,69

For the static quenching, the formation of a complex in the ground state, it is not observed a decrease in the decay times because only the unquenched fluorophores fluorescence is observed. In the case of dynamic quenching, it is observed a decrease in the decay times because is a rate process acting on the entire excited-state population [92]. In this case, is observed that τ_2 is more dominant than τ_1, and the value of τ_2 does not vary, so, the mechanism would be static. To confirm this hypothesis, the K_q values are calculated by the following equation:

$$K_{SV} = K_q \tau_0 \tag{8}$$

Where K_{sv} is Stern-Volmer constant, K_q is the bimolecular quenching constant, and τ_0 is the lifetime of the fluorophore in the absence of quencher [76]. The values of the K_q are represented in the **Table 12**. It is observed that the k_q values are higher than the maximum diffusion rate constant in water ($k_{diff} \approx 7.40 \times 10^9$ $M^{-1} s^{-1}$ at 298K, according to Smoluchowski-Stokes-Einstein theory at 298K), so the quenching is static, the association occur in the ground-state [96].

Table 12. K_{sv} and K_q values of TDF, TFV and AZT.

Molecule	T^o K	K_{sv} ($\times 10^3$) Lmol^{-1}	τ_0 ($\times 10^{-9}$) s	k_q ($\times 10^{11}$) Lmol^{-1}s^{-1}
TDF	289,15	2.146	6	3.58
	296,15	2.053	6	3.42
	303,15	2.070	6	3.45
	310,15	1.915	6	3.19
TFV	289,15	2.247	6.16	3.65
	296,15	2.037	6.16	3.31
	303,15	2.068	6.16	3.36
	310,15	1.913	6.16	3.11
AZT	289,15	3.196	6.11	5.23
	296,15	3.200	6.11	5.24
	303,15	3.194	6.11	5.23
	310,15	3.458	6.11	5.66

3.5. Isothermal titration calorimetry (ITC) analysis

The last experiment was the Isothermal titration calorimetry or ITC. The ITC is a biophysical technique for measuring the formation and dissociation of molecular complexes. The ITC it´s based on the measure of the heat absorbed or released during bond formation, providing accurate, rapid, and label-free measurement of the thermodynamics of molecular interaction [97]. The ITC instrument is a heat-flux calorimeter operating according to the dynamic power compensation principle, it measures the amount of power (μcal/sec) required to maintain a constant temperature difference (close to zero) between the sample and the reference cell. With this heat the thermodynamic parameters and the K are obtained [98]. The experiments only were done at 289,15K because at a higher temperature the albumin formed aggregates.

The plots obtained with this technique appear represented in the **Figure 18** to the interaction HSA-TFV and HSA-AZT, the rest of the cases are in the **Figure 3** of the **Appendix**. It is observed that the tenofovir plots, HSA-TFV and HSA-TDF, have the peaks under the zero, it means that the interactions are exothermic, release heat; however, the HSA-AZT, HSA-FCT and HSA-3TC plots have the peaks above the zero, so the interactions are endothermic, absorb heat. It is observed in all the plot that the heat release and absorbed are very small, so the data obtained with ITC (at the experimental condition done) may not have a high degree of reliability.
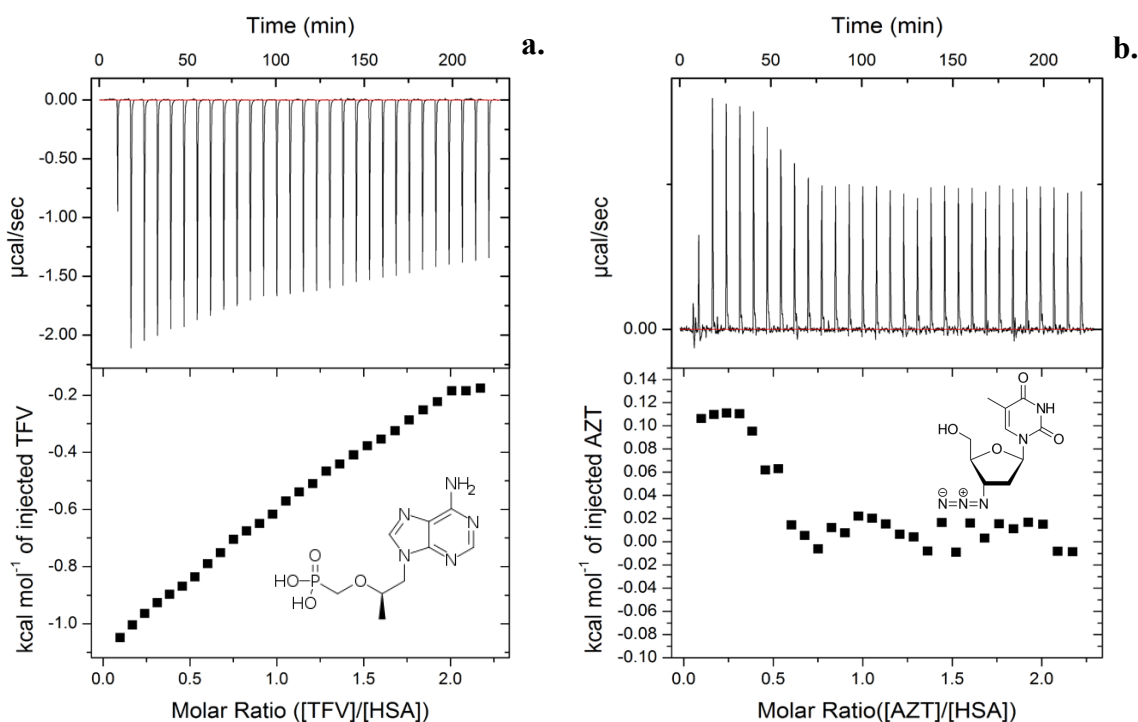
Figure 18. Calorimetry titration of HSA-TFV (**a**) and HSA-AZT (**b**).

From ITC plots the K values and thermodynamic parameters represented in the **Table 13** were obtained. The values of K obtained are higher than the K_a obtained from steady-state fluorescence experiments. Steady-state fluorescence experiment led us to conclude that the interactions between the HSA and all the antiretrovirals are weak, which corresponds to low K values (10^3). ITC obtained values would lead to the conclusion that at least some of the antiretrovirals had stronger bonding (more extensive complex formation, high valor of K). The n values are near to 1, the interaction occur when the stoichiometry is 1:1. But it is interesting to observe that the ΔH, ΔS and ΔG have the same sign that in the Steady-State fluorescence, confirming that the interactions between HSA-TFV and HSA-TDF are exothermic and the interactions between HSA-FCT, HSA-3TC and HSA-AZT are exothermic (it can see in the ITC plots); and all the interactions are spontaneous.

Table 13. K and n values and thermodynamic parameters obtained with ITC for the HSA.

Interaction	K (x10^3) Lmol^{-1}	n	$\Delta H°$ kJmol^{-1}	$\Delta S°$ Jmol^{-1}K^{-1}	$\Delta G°$ kJmol^{-1}
HSA-TFV	12.3±0.985	1.24±0.02	-5.54±0.15	0.059	-22.6
HSA-TDF	9.60±0.84	1.05±0.24	-5.94±0.24	0.056	-22.1
HSA-FCT	454±135	0.703±0.017	0.28±0.01	0.109	-31.24
HSA-3TC	19.6±6.79	0.215±0.122	2.46±1.45	0.091	-23.84
HSA-AZT	675±424	0.474±0.024	4.81±0.03	1.13	-321.9

The same experiment was realized to the g-HSA-AZT, obtaining the plot represented in the **Figure 19**. It observed that the interaction is endothermic, and the heat absorbed is also very small.
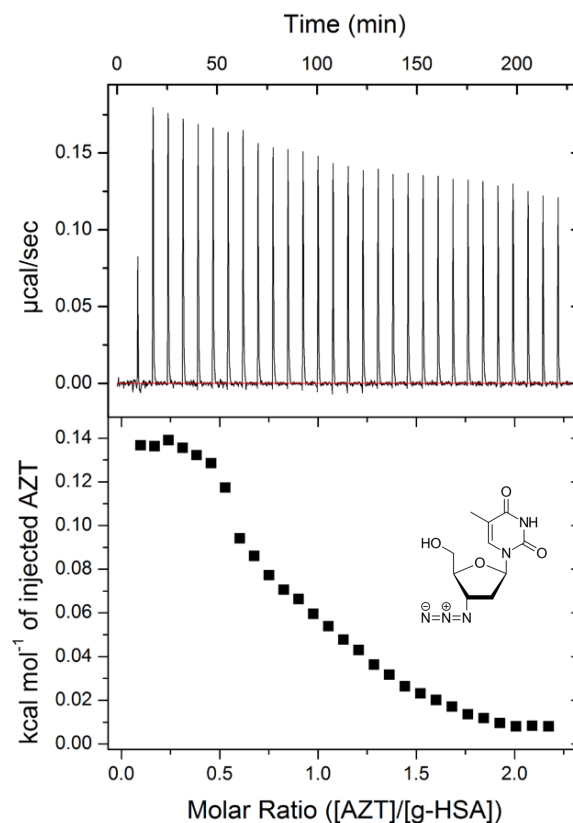
Figure 19. Calorimetry titration gHSA-AZT.

The K_a values and thermodynamic parameters obtained to the ITC plot are represented in the **Table 14.** It observed the same things that in the case of HSA, the K value are very big in comparison with the K obtained from steady-state fluorescence. The n indicates that the stoichiometry is 1:1. And the thermodynamic parameters confirm that the interaction is endothermic ($\Delta H > 0$) and spontaneous ($\Delta G < 0$), thus, entropically directed.

Table 14. K and n values and thermodynamic parameters obtained with ITC for the g-HSA.

Interaction	$K(x10^3)$ $Lmol^{-1}$	n	$\Delta H°$ $kJmol^{-1}$	$\Delta S°$ $Jmol^{-1}K^{-1}$	$\Delta G°$ $kJmol^{-1}$
gHSA-AZT	61.4±8.19	0.866±0.023	0.72±0.023	0.009	-25.3

CHAPTER 4: CONCLUSION AND FUTURE WORK

The interactions between HSA-antiretrovirals and BSA-antiretrovirals are weak, the values of K_{sv} are very low, from the order of 10^3 M^{-1}. The values of n are near to 1, its indicates that the stoichiometry between the albumins and the antiretrovirals is 1:1 and only exists one local the interaction. In all the cases the values of ΔG are negatives, so the interactions are spontaneous. The other thermodynamic parameters may vary depending on de interaction: for most of the antiretrovirals albumins the interactions ΔH and ΔS are >0, so, these interactions are endothermic (occur with absorption of heat) and are entropically directed, the principally forces of interaction in these cases are hydrophobic [68]. HSA-TDF, HSA-TFV and BSA-3TC ΔH<0 and ΔS>0, so, these interactions are exothermic (occur with release of heat), and the principally interaction forces are electrostatic [71];

It is observed that the K_{sv} values with the g-HSA-FCT/AZT are bigger than in the case of HSA or BSA, but not significantly, its indicated that the interactions with the glycated albumin maybe are more favored due to some change in the structure which will facilitate the binding between the antiretrovirals and the g-HSA, and this part will be studied in the future to know for sure which is this difference which enables that the interaction be favored and will be performed the same experiments to the other antiretrovirals to see if they show the same tendence. The two studied antiretrovirals with the g-HSA have a ΔG°<0, so the interactions are spontaneous. The other values of thermodynamic parameters are ΔH° and a ΔS° >0, so the processes are endothermic (confirmed with the ITC results), entropically directed, and the principally forces of interaction are hydrophobic.

With the Time-resolved fluorescence is observed that the lifetimes don´t vary with the increased of the antiretroviral concentration, so the mechanism of the interaction between the HSA and the three tested antiretrovirals (TDF, TFV and AZT) is a static quenching. As a future perspective is necessary to do the same experiments for the other antiretrovirals.

The ITC results indicate that the heat absorbed or released are very low, so the constants values and the thermodynamic parameters absolute values are not comparable with the Steady-state fluorescence results. Even considering that fact, the ITC technique confirmed that the processes are exothermic (in the case of HSA-TDF, HSA-TFV and BSA-3TC) and endothermic (in the rest of the cases). To improve the results the ITC experiment will have to repeated in other conditions, for example, increasing the concentration. The only thing this method confirmed is if the interactions are endothermic or exothermic, and these results agree with the fluorescence results.

As a preliminary conclusion we advance that the steady-state fluorescence provides more reliable data than ITC when the heat release or absorbed is too low. The same interactions will be studied in other conditions and with other methods to complete the results obtained so far.

REFERENCES

1 Haase, A. T. Pathogenesis of lentivirus infections. Nature, 1986; 3222 (6075), 130-136

2 Dubois, N. et al. Retroviral RNA Dimerization: From Structure to Functions. Front Microbiol, 2018 (Review)

3 Longo, D.L. et al. Los retrovírus humanos. (https://accessmedicina.mhmedical.com/content.aspx?bookid=1717&sectionid=114923877#har19_c225e_tbl001) (accessed on 26 March 2022)

4 ONUSIDA. Available online: https://www.unaids.org/es/resources/fact-sheet (accessed on 26 March 2022).

5 Human Immunodeficiency Virus (HIV). Transfus Med Hemother: offizielles organ der Deutschen Gesellschaft fur Transfusionsmedizin und Immunhamatologie, 2016, 43 (3), 203-222.

6 Centros para el Control y la Prevención de Enfermedades. Available online: https://www.cdc.gov/hiv/spanish/basics/index.html (accessed on 19 March 2022).

7 Peruski, A. H. et al. Trends in HIV-2 Diagnoses and Use of the HIV-1/HIV-2 Differentiation Test-United States, 2010-2017. MMWR Morb Mortal Wkly Rep, 2020; 69, 63-66

8 National Library of Medicine. Available online: https://medlineplus.gov/lab-tests/cd4-lymphocyte-count/ (accessed on 26 March 2022).

8 Peruski, A. H. et al. Trends in HIV-2 Diagnoses and Use of the HIV-1/HIV-2 Differentiation Test-United States, 2010-2017. MMWR Morb Mortal Wkly Rep, 2020; 69, 63-66

9 Tang, J.W. et al. The basis of HIV Medicine (https://www.aids.gov.hk/pdf/g190htm/01.htm)(accessed on 26 March 2022)

10 Fiorentini, S. et al. Functions of the HIV-1 matrix protein p17. New Microbiol, 2006; 29 (1), 1-10

11 Rosi, E. et al. Structure, Function, and Interactions of the HIV-1 Capsid Protein. Life, 2021; 11(2), 100.

12 Gien, H. et al. Nucleocapsid Protein Binds Double-Stranded DNA in Multiple Modes to Regulate Compaction and Capsid Uncoating. Viruses, 2022; 14, 235.

13 Tian, L. et al. Structure of HIV-1 reverse transcriptase cleaving RNA in an RNA/DNA hybrid. Proc Natl Acad Sci, 2018; 115, 507-512

14 Craige, R. The molecular biology of HIV integrase. Future Virol, 2012; 7 (7), 679-686.

15 Gulnik, S. HIV protease: enzyme function and drug resistance. Vitam Horm, 2000; 58, 213-256.

16 Rose, K. M. el al. The viral infectivity factor (Vif) of HIV-1 unveiled. Trends Mol Med, 2004; 10 (6), 291-297.

17 Muthumani, K. et al. Mechanism of HIV-1 viral protein R-induced apoptosis. Biochem Biophys Res Commun, 2003; 304 (3), 583-592.

18 Fritz, J. V. et al. HIV-1 viral protein r: from structure to function. Future Virol, 2010; 5 (5) (Review)

19 Lijima, K. et al. Viral protein R of human immunodeficiency virus type-1 induces retrotransposition of long interspersed element-1. Retrovirology, 2013; 10 (83)

20 Joseph, A. M. el al. Nef: "Necessary and Enforcing Factor" in HIV Infection. Current HIV research, 2005; 3 (1), 87-94.

21 Pallesen, J. et al. Structure of the HIV-1 Rev response element alone and in complex with regulator of virion (Rev) studied by atomic force microscopy. FEBS J, 2009; 276 (15), 4223-4232.

22 Clark, E. et al. Tat is a multifunctional viral protein that modulates cellular gene expression and functions. Oncotarget, 2017; 8, 27569-27581.

23 RCSB Protein Data Bank. Available online: https://cdn.rcsb.org/pdb101/learn/resources/structural-biology-of-hiv/index.html# (accessed on 21 March 2022).

24 Wilen, C. B. HIV: Cell Binding and Entry. Cold Spring Harb Perspect Med, 2012; 2 (8).

25 Hu, W.S. et al. HIV-1 Reverse Transcription. Cold Spring Harb Perspect Med, 2012; 2 (10).

26 Craigie, R. et al. HIV DNA Integration. Cold Spring Harb Perspect Med, 2012; 2 (7).

27 Roebuck, K. A. et al. Regulation of HIV- Transcription. Gene Expr, 1999; 8 (2), 67-84.

28 Burugu, S. et al. HIV-1 translation and its regulation by cellular factors PKR and PACT. Virus Res, 2014, 193, 65-77.

29 Sundquist, W. I. et al. HIV-1 Assembly, Budding and Maturation. Cold Spring Harb Perspect Med, 2012; 2 (7).

30 NIAID: National Institute of Allergy and Infectious Diseases. Available online: https://www.flickr.com/photos/niaid/5057022555/in/album-72157625994990013/ (accessed on 21 March 2022).

31 Medical News Today: ¿Cómo funciona la terapia antirretroviral? Available online: https://www.medicalnewstoday.com/articles/es/medicamentos-antirretrovirales-para-el-vih (accessed on 4 April 2022).

32 Lv, Z. et al. HIV Protease Inhibitors: a review of molecular selectivity and toxicity. HIV/AIDS (Auckl), 2015; 7, 95-104.

33 Wang, X. et al. Molecular Mechanisms of HIV Protease Inhibitor-Induced Endothelial Dysfunction. JAIDS, 2007; 44 (5), 493-499.

34 Tilton, C. T. et al. Entry inhibitors in the treatment of HIV-1 infection. Antiviral Res, 2010; 85 (1), 91-100.

35 ASHM: Antiretrovrial drugs and other therapies in HIV patients. Available online: https://hivmanagement.ashm.org.au/antiretroviral-drugs/hiv-entry-inhibitors/ (accessed on 8 April 2022).

36 ChemicalBook. Available online: https://m.chemicalbook.com/ChemicalProductProperty_EN_CB7358557.htm (accessed on 8 April 2022).

37 Blanco, J. L. et al. HIV integrase inhibitors: a new era in e treatment of HIV. Expert Opinion on Pharmacotherapy, 2015; 16 (9), 1313-1324.

38 Patel, P. H et al. Reverse Transcriptase Inhibitors. StatPearls, 2022.

39 Ren, L. et al. Structure of HIV-2 reverse transcriptase at 2.35-Å resolution and the mechanism of resistance to non-nucleoside inhibitors. Biol Sci, 2002; 99 (22), 14410-14415

40 Hall, A. M. et al. Tenofovir-Associated Kidney Toxicity in HIV-Infect Patients: A Review of the Evidence. Am J Kideny Dis, 2011; 11 (5), 773-780.

41 Fung, H. P. et al. Tenofovir Disoproxil Fumarate: A Nucleotide Reverse Transcriptase Inhibitor for the Treatment of HIV Infection. Clin Ther, 2002; 24 (10), 1515-1548.

42 Mesquita, P. M. M. et al. Intravaginal ring delivery of tenofovir disoproxil fumarate for prevention of HIV and herpes simplex virus infection. J Antimicrob Chemoter, 2012; 67 (7), 1730-1738.

43 Ray, A. S. et al. Tenofovir alafenamide: A novel prodrug of tenofovir for the treatment of Human Immunodeficiency Virus. Antiviral Res, 2015; 125.

44 Saravolatz, L. D. et al. Emtricitabine, a New Antiretroviral Agent with against HIV and Hepatitis B Virus. Clin Infect Dis, 2006; 42 (1), 126-131.

45 Bang, L. M. et al. Emtricitabine. Drugs, 2003; 63, 2413-2424.

46 Aidsmap. Available online: https://www.accessdata.fda.gov/drugsatfda_docs/label/2008/021500s010,021896s004lbl.pdf (accessed on 12 April 2022).

47 Quercia, R. et al. Twenty-Five Years of Lamivudine: Current and Future Use for the Treatment of HIV-1 Infection. J Acquir Immune Defic Syndr, 2018; 78 (2), 125-135.

48 Santiago, B. I. F. et al. Antiviral and Cellular Metabolism Interactions between Dexelvucitabine and Lamivudine. Am Soc Microbiol, 2007; 51 (6)

49 Veal, G. J. et al. Metabolism of Zidovudine. Gen Pharmac, 1995; 26 (7), 1469-1475.

50 Fanali, G. et al. Human serum albumin: From bench to bedside. Mol Aspects Med, 2012; 33 (3), 209-290.

51 Sugio, S. et al. Crystal structure of human serum albumin at 2,5 Å resolution. Protein Eng Des Sel, 1999; 12 (6), 439-446.

52 Fasano, M. et al. The extraordinary Ligand Binding Properties of Human Serum Albumin. Life, 2005; 57 (12), 787-796.

53 Moman, R. N. et al. Physiology Albumin. StatPearls, 2022.

54 Bujacz, A. Structure of bovine, equina and leporine serum albumim. Acta Crystallogr D Biol Crystallogr, 2012; 68 (10), 1278-1289.

55 Naveenraj, S. et al. Binding of serum albumins with bioactive substances - Nanoparticles to drugs. J Photochem Photobiol C: Photochem Rev, 2013; 14, 53-71.

56 Nicholson, J. P.et al. The role of albumin in critical illness. Br J Anaesth, 2000; 85, 599-610.

57 Gelamo, E. L. et al. Interaction of bovine (BSA) and human (HSA) serum albumins with ionic surfactants: spectroscopy and modelling. Biochim Biophys Acta, 2002; 1594, 84-99.

58 Yamasaki, K. et al. Characterization of site I on human serum albumin: concept about the structure of a drug binding site. Biochim Biophys Acta, 1996; 1295, 147-157.

59 Deeb, O. et al. Exploration of human serum albumin binding sites by docking and molecular dynamics flexible ligand-protein interactions. Biopolymers, 2009; 93 (2), 161-170.

60 Wani, T. A. et al. Study of Interactions o an Anticancer Drug Neratinib With Bovine Serum Albumin: Spectroscopic and Molecular Docking Approach. Front Chem, 2018; 6, 2296-2646.

61 Zsila, F. Subdomain IB Is the Third Major Drug Binding Region of Human Serum Albumin: Toward the Three-Sites Model. Mol Pharm, 2013; 10, 1668-1682.

62 Taylor, S. I. et al. Insulin resistance or insulin deficiency: which is the primary cause of NIDDM? Diabetes, 1994; 43 (6), 735-740.

63 Wilcox, G. Insulin and Insulin Resistance. Clin Biochem Rev, 2005; 26 (2), 19-39.

64 Anguizola, J. et al. Review: Glycation of human serum albumin. Clin Chim Acta, 2013; 425, 64-76.

65 Joseph, K. S. et al. Binding of tolbutamide to glycated serum albumin. J Pharm Biomed Anal, 2011; 54 (2), 426.432.

66 Qiu, H. Y., et al. Comprehensive overview of human serum albumin glycation in diabetes mellitus. World J Diabetes, 2021; 12 (7), 1057-1069.

67 Arasteh, A. et al. Glycated albumin: an overview of the *In Vitro* models of an *In Vivo* potential disease marker. J Diabetes Metab Disord, 2014; 13, 49.

68 Alanazi, A. M., et al. Unraveling the binding characteristics of the anti-HIV agents abacavir, efavirenz and emtricitabine to bovine serum albumin using spectroscopic and molecular simulation approaches. J Mol Liq, 2018; 251, 345-357.

69 Shi, J. M. et al. Multi-spectroscopic and molecular modeling approaches to elucidate the binding interaction between bovine serum albumin and darunavir, a HIV protease inhibitor. Spectrochim Acta A Mol Biomol Spectrosc, 2018; 188, 362-371.

70 Patnin, S. et al. Binding interaction of potent HIV-1 NNRTIs, amino-oxy-diarylquinoline with the transport protein using spectroscopic and molecular docking. Spectrochim Acta A. Mol Biomol Spectrosc, 2020; 233, 118159.

71 Tunç. S. et al. Studies on the interactions of chloroquine diphosphate and phenelzine sulfate drugs with human serum albumin and human hemoglobin proteins by spectroscopic techniques. J Lumin, 2013; 140, 87-94.

72 https://www.wavefun.com/, accessed in July 2022.

73 https://www.ccdc.cam.ac.uk/solutions/csd-discovery/components/gold/, accessed in July 022.

74 https://pymol.org/2/ accessed in July 2022.

75 Chaves, O. A. et al. Evaluation by fluorescence, STD-NMR, docking and semi-empirical calculations of the o-NBA photo-acid interaction with BSA. Spectrochim Acta A. Mol Biomol Spectrosc, 2016; 169, 175-181.

76 Lakowicz, J. R. Principles of fluorescence spectroscopy, 3rd ed. Springer, New York, 2006.

77 Chaves, O. A. et al. Fluorescence and docking studies of the interaction between human serum albumin and pheophytin. Molecules, 2015; 20, 19526-19539.

78 Zaidi, N. et al. A comprehensive insight into binding of hippuric acid to human serum albumin: A study to uncover its impaired elimination through hemodialysis, PLoS ONE, 2013; 8, e71422.

79 Moreno, M. J. et al. Analysis of the Equilibrium Distribution of Ligands in Heterogeneous Media–Approaches and Pitfalls. Int J Mol Sci, 2022; 23, 9757.

80 Weert, M. et al. Fluorescence quenching and ligand binding: A critical discussion of a popular methodology. J Mol Struct, 2011; 998, 144-150.

81 J. Pina, et al. Alternating binaphthyl−thiophene copolymers: synthesis, spectroscopy, and photophysics and their relevance to the question of energy migrationversus conformational relaxation, Macromolecules, 2009: 42, 1710-1719.

82 G. Striker, et al. Photochromicity and fluorescence lifetimes of greenfluorescent protein. J Phys Chem B, 1999; 103, 8612-8617.

83 Samelo, J. et al. Partition of Amphiphilic Molecules to Lipid Bilayers by ITC: Low-Affinity. ACS Omega, 2017; 2 (10), 6863-6869.

84 Sudlow, G., et al. Further characterization of specific drug binding sites on human serum albumin. Mol Pharmacol, 1976; 12, 1052–1061.

85 Acunha, T. V. et al. Fluorescent pyrene moiety in fluorinated C 6 F 5 -corroles increases the interaction with HSA and CT-DNA, J. Porphyr. Phthalocyanines, 2021; 25, 75-94.

86 Manjushree, M. et al. Interpretation of the binding interaction between bupropion hydrochloride with human serum albumin: A collective spectroscopic and computational approach, Spectrochimica Acta Part A, 2019; 209, 264–273.

87 Naik, P. N. et al. Non-covalent binding analysis of sulfamethoxazole to human serumalbumin: Fluorescence spectroscopy, UV–vis, FT-IR, voltammetric and molecular modeling. J Pharmac, 2015; Anal. 5, 143–152.

88 Zhang, W. et al. Spectroscopic and molecular docking studies on the interaction of dimetridazole with human serum albumin. J Chil Chem Soc, 2013; 58, 1717-1721.

89 Acunha, T. V. et al. Fluorescent pyrene moiety in fluorinated C 6 F 5 -corroles increases theinteraction with HSA and CT-DNA. J Porphyr, Phthalocyanines, 2021; 25, 75-94.

90 Zhu, M. et al. Biointeractions of herbicide atrazine with human serum albumin: UV-vis, fluorescence and circular dichroism approaches. Int J Environ Res Public Health, 2018; 15, 116.

91 Manjunath, S. et al. Nature of autofluorescence in human serum albumin under its native, unfolding and digested forms. Proc SPIE 8935, Advanced Biomedical and Clinical Diagnostic Systems XII, 2014; 893620.

92 Yildirim, B. et al. Fluorescence interactions of a novel chalcone derivative with membrane model systems and human serum albumin. Byophys Chem, 2022; 290.

93 Huang, Z. Y. et al. Comparative study of two antipsychotic drugs binding to human serum albumin: by multispectroscopic and molecular docking methods. J Mol Liq, 2022; 365.

94 Amiri, M. et al. Origin of fluorescence lifetimes in human serum albumin. Studies on native and denatured protein. J Fluoresc, 2010; 20, 651–656

95 Chaves, O. A. et al. Biophysical Characterization of the Interaction between a Transport Human Plasma Protein and the 5,10,15,20-Tetra(pyridine-4-yl)porphyrin. Mol, 2022; 27 (16), 5341.

96 Montalti, M. et al. Handbook of photochemistry. CRC Press, Taylor & Francis, 2006; 3rd edition.

97 Ghai, R. et al. Applications of isothermal titration calorimetry in pure and applied research-survey of the literature from 2010. J Mol Recognit, 2011; 25 (1), 32-52.

98 Velazquez-Campoy, A. et al. Isothermal Titration Calorimetry. Current protocols in cell biology. editorial board, Juan S. Bonifacino ... [et al.], 2004; 17 (17.8).

APPENDIX

Table 1. Name, abbreviation, and structure of all antiretrovirals.
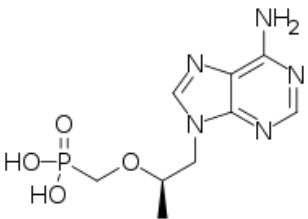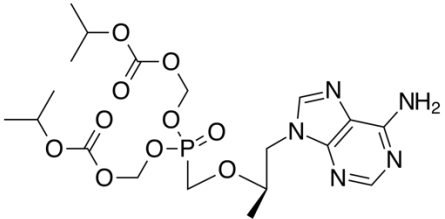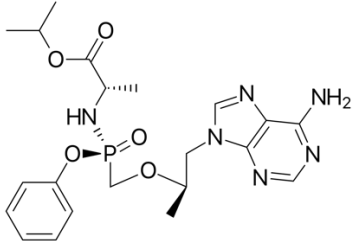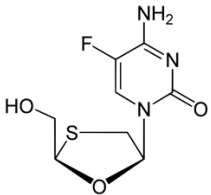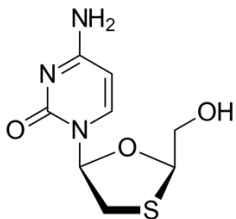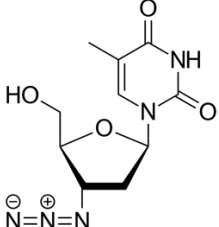
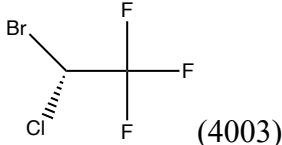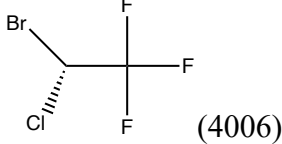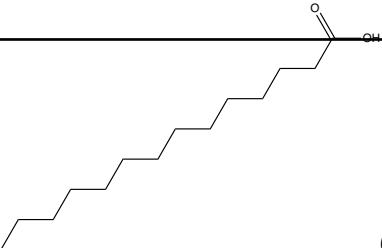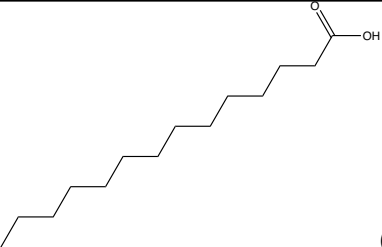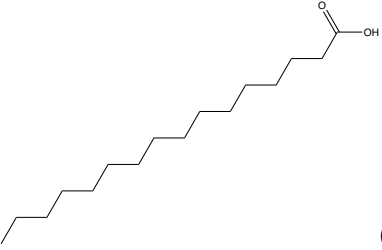| ANTIRETROVIRAL	ABBREVIATION	STRUCTURE
Tenofovir	**TFV**	
Tenofovir Disoproxil Fumarate	**TDF**	
Tenofovir Alafenamide	**TAF**	
Emtricitabine	**FCT**	
Lamivudine	**3TC**	
Zidovudine	**AZT**	
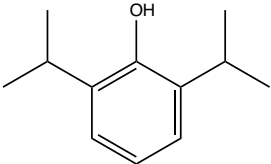
Table 2. Results of RMSD with 1N5U like mother molecule.
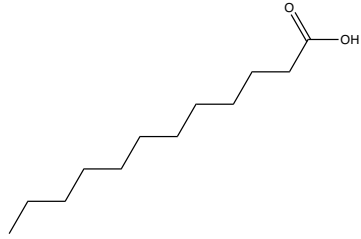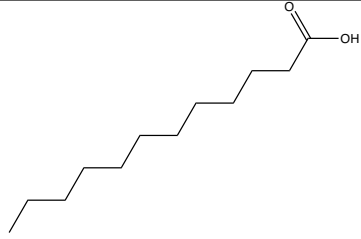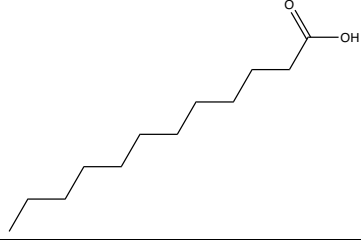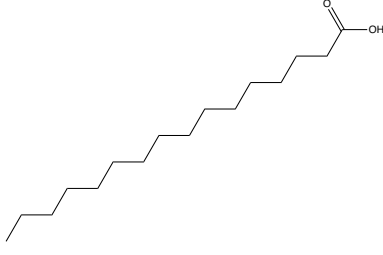
Mother molecule	B molecule	Align RMSD value	Cealign RMSD value	Super RMSD value
1N5U	4L9O	4.050	5.189	**3.755**
1N5U	4L9K	**3.637**	4.825	3.655
1N5U	6WUW	**0.610**	0.715	**0.610**
1N5U	4L8U	**0.212**	0.281	**0.212**
1N5U	6EZQ	3.320	4.261	**3.251**
1N5U	2BXA	3.003	4.632	**2.915**
1N5U	2BXH	3.174	4.822	**3.123**
1N5U	4E99	**3.869**	5.289	**3.869**
1N5U	2BXP	**0.519**	0.582	**0.519**
1N5U	2VUE	3.273	4.713	**3.239**
1N5U	1E7A	3.392	4.926	**3.360**
1N5U	1E7B	3.326	5.024	**3.301**
1N5U	1E7C	**0.763**	0.784	**0.763**
1N5U	1E7F	0.697	0.751	**0.696**
1N5U	1E7H	**0.701**	0.864	**0.701**
1N5U	1GNI	0.639	0.732	**0.638**
1N5U	2XWO	**2.984**	4.547	2.995
1N5U	6HSC	**0.510**	0.620	**0.510**
1N5U	2BXK	**0.630**	0.676	**0.630**
Results		**11**	0	**16**
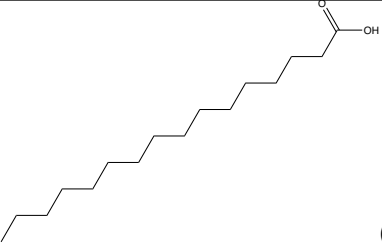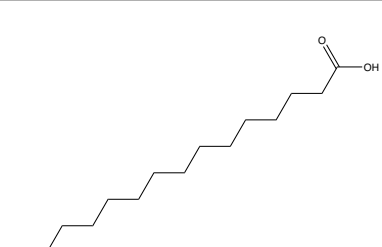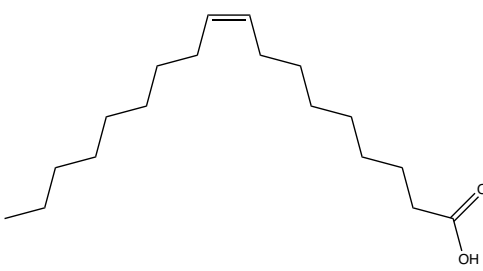
Table 3. Results of RMSD with 6HSC like mother molecule.

Mother molecule	B molecule	Align RMSD value	Cealign RMSD value	Super RMSD value
6HSC	4L9O	3.888	4.792	**3.822**
6HSC	4L9K	3.416	4.663	**3.375**
6HSC	6WUW	**0.590**	0.600	**0.590**
6HSC	4L8U	**0.452**	0.554	**0.452**
6HSC	6EZQ	3.176	4.051	**3.096**
6HSC	2BXA	2.822	4.371	**2.795**
6HSC	2BXH	2.954	4.522	**2.909**
6HSC	4E99	**3.706**	5.206	**3.706**
6HSC	2BXP	**0.601**	0.638	**0.601**
6HSC	2VUE	**3.034**	4.539	**3.034**
6HSC	1E7A	3.170	4.694	**3.163**
6HSC	1E7B	3.147	4,746	**3.081**
6HSC	1E7C	**0.850**	0.856	**0.850**
6HSC	1E7F	**0.815**	0.822	**0.815**
6HSC	1E7H	**0.936**	0.993	**0.936**
6HSC	1GNI	**0.768**	0.849	**0.768**
6HSC	2XWO	**2.822**	4.364	2.824
6HSC	1N5U	**0.510**	0.620	**0.510**
6HSC	2BXK	**0.718**	0.746	**0.718**
Results		**12**	0	**19**
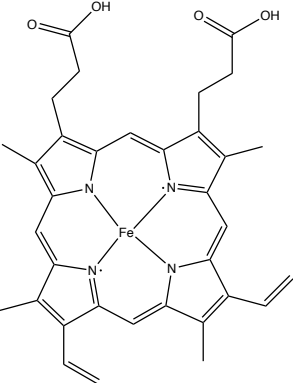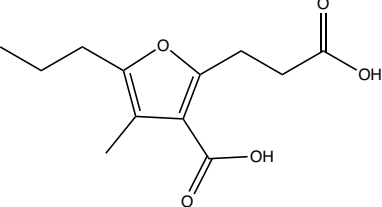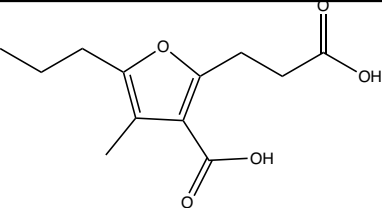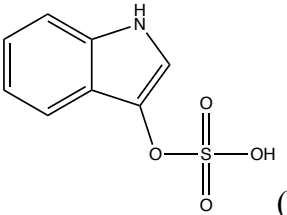
Table 4. Results of redocking analysis.
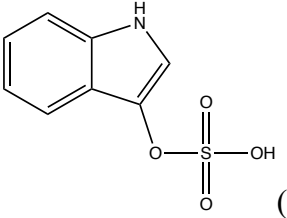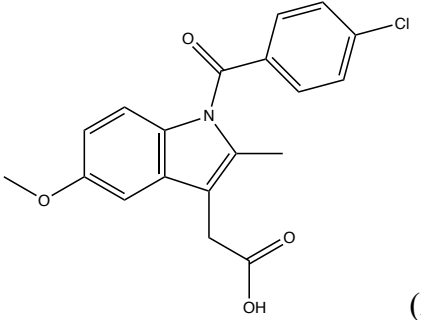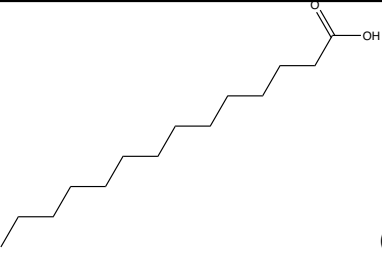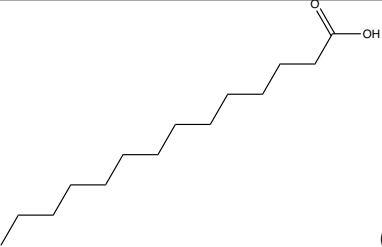
PDB code	Resolution/Å	Ligand	Ligand site	RSMD ChemPLP	RSMD ChemScore	RSMD ASP
1E7A	2,20		II	0.6873	0.9941	2.4064
1E7B	2,38	(4003)	II	erro	erro	erro
1E7C	2,40	(4006)	I	erro	erro	erro
		(1004)	II	1.8599	1.9139	0.9679
		(1001)	III	1.5229	1.0905	1.2899
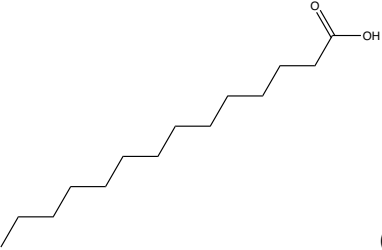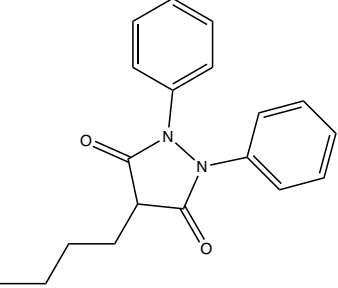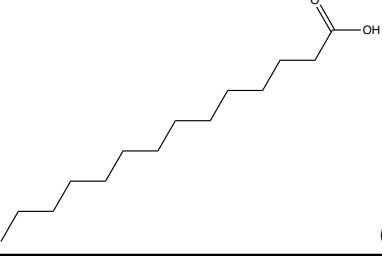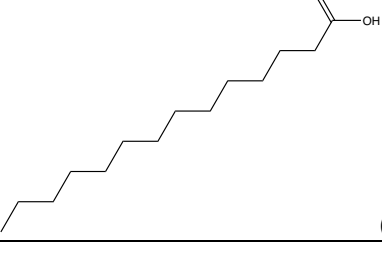
1E7F	2,43	(1007)	I	2.1310	1.9833	3.9574
		(1004)	II	0.9735	1.0664	0.9058
		(1001)	III	1.3722	1.3663	1.3978
1E7H	2,43	(1006)	I	2.2155	1.7274	1.8913
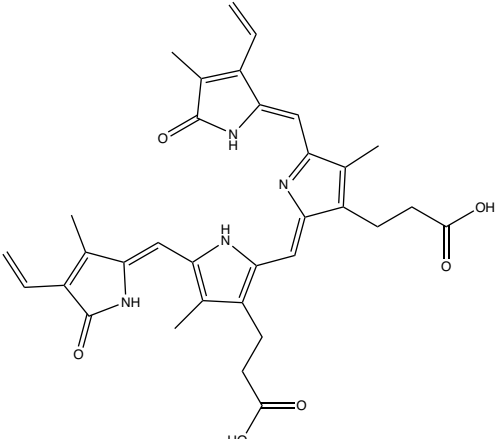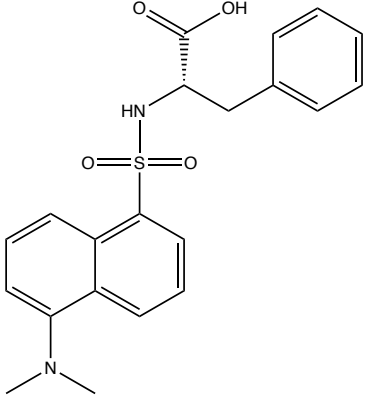
1E7H	2,43	(1007)	I	6.1425	1.9695	6.5280
		(1004)	II	1.7476	1.3815	1.4592
		(1001)	III	0.9216	1.3139	1.1867
1GNI	2,40	(1007)	I	4.2767	3.3673	4.5001
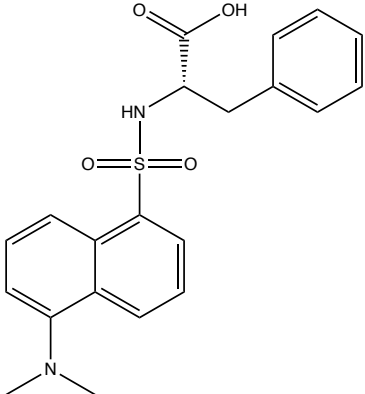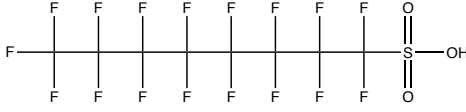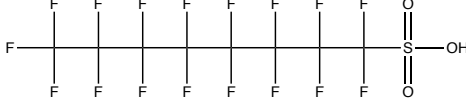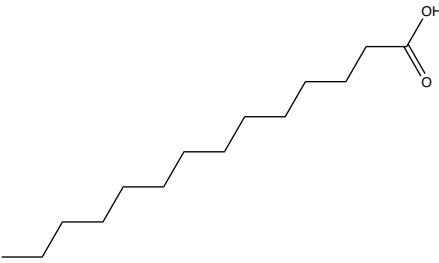
1GNI	2,4	(1004)	II	1,1649	1.7187	1.1610
		(1001)	III	1.4314	1.4354	1.2684
1N5U	1,90	(1006)	I	2.7885	9.3455	8.4391
		(1004)	II	1.6330	1.5510	1.0793
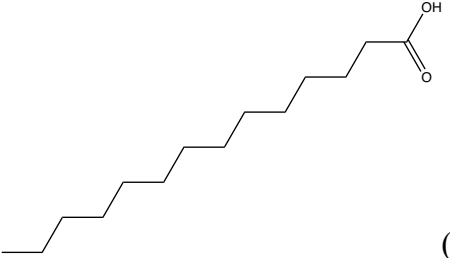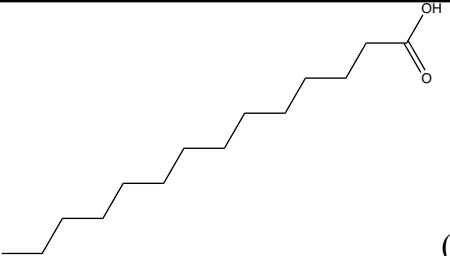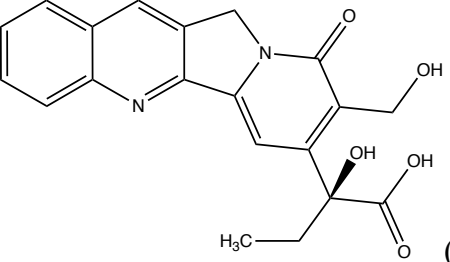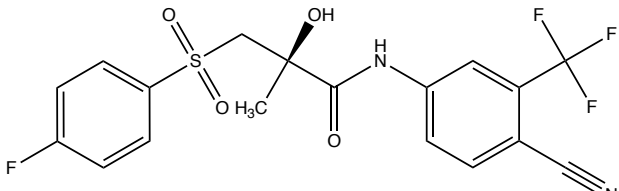
1N5U	1,90	(605)	III	0.5831	0.7960	0.5078
2BXA	2,35	(2001)	I	0..6973	0.9392	0.7752
		(2002)	II	0.7416	0.7211	0.9581
2BXH	2,25	(1002)	I	4.4424	4.2719	4.2948
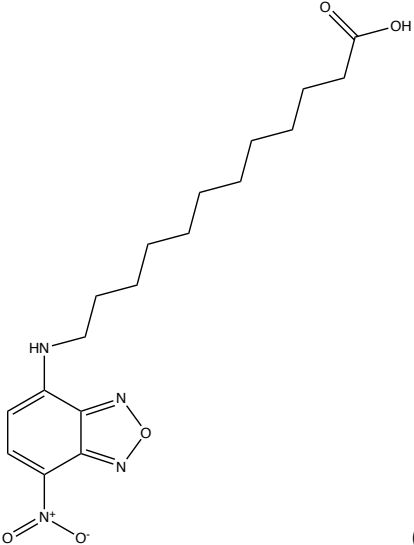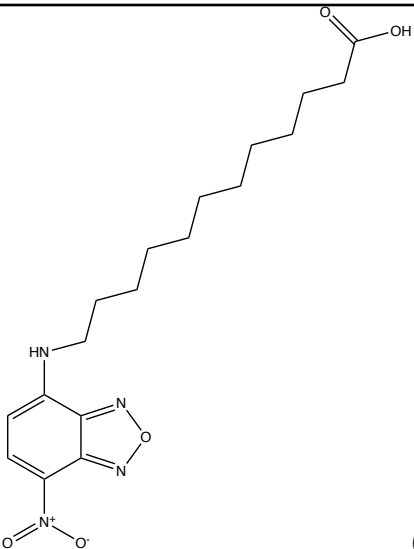
2BXH	2,25	(1001)	II	0.2221	0.2089	0.3651
		(2001)	I	0.6061	0.7730	0.4240
2BXK	2,40	(1004)	II	1.1412	1.0311	0.8194
		(1001)	III	1.3330	1.3663	1.3694
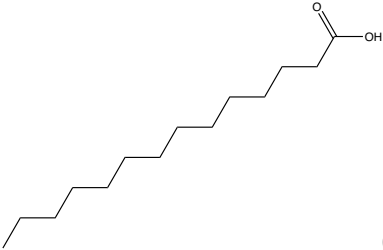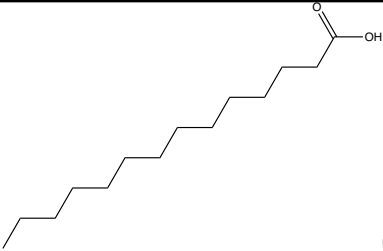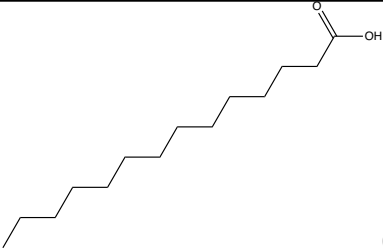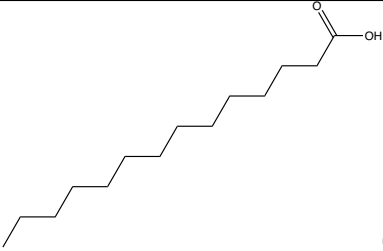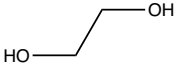
2BXP	2,30	(1009)	I	1.8162	2.0341	1.1808
		(3001)	I	0.4851	0.4221	0.4729
		(1004)	II	1.4044	1.4623	2.3578
		(1001)	III	1.3381	1.1228	1.3280

2VUE	2,42		III	3.8349	1.6068	4.9521
2XW0	2,40	 (2002)	I	5.0687	2.4670	1.9880

2XW0	2,40	(2001)	II	0.7290	0.8941	0.6264
4E99	2,30	(602)	I	8.3212	8.1278	6.9607
		(601)	II	10.5606	11.3517	1.3767
4L8U	2,01	(605)	I	1.8632	1.6922	8.8711
	2,01					

4L8U		(603)	II	0.9326	0.9265	0.6305
		(606)	III	0.7676	0.4497	0.5474
4L9K	2,40	(601)	III	0.5971	0.7846	0.6750
4L90	2,40		III	4.7407	7.3261	7.4579

| 6EZQ | 2,39 | (601) | I | 2.8290 | 2.7307 | 3.8379 |
| | | (602) | II | 2.3441 | 2.5860 | 2.3681 |

6HSC	1,90	 (605)	I	10.1197	10.3465	10.4970
		 (607)	I	3.9309	4.2121	4.0268
		 (602)	II	1.5663	1.2643	1.2720
		 (606)	III	1.3468	1.3441	1.1912
6WUW	2,20	 (607)	I	1.9112	1.6552	1.7296
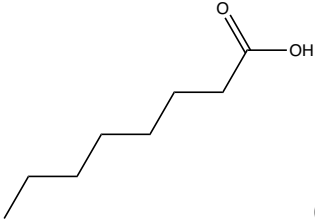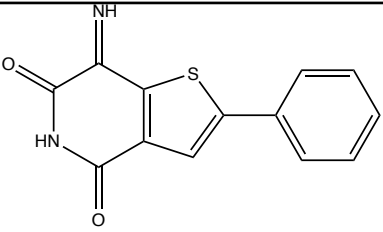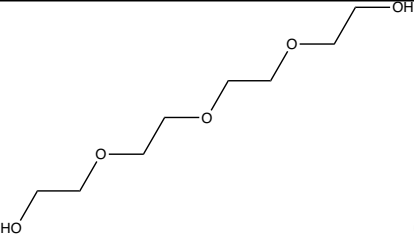
6WUW	2,20	(604)	II	1.6707	1.4728	1.1162
		(602)	III	0.5748	2.4745	2.4111
		(606)	III	1.2377	1.2785	1.2308
Results				12	18	17

Table 5. Results of docking molecular analysis.

PROTEIN	ANTIRETROVIRAL	SITE I	SITE II	SITE III
1E7A	Tenofovir Disoproxil Fumarate	26.3529	23.8100	26.1349
	Tenofovir	18.9556	18.0075	19.4105
	Tenofovir alafenamide	26.9130	29.9482	30.2114
	Emtricitabine	15.6961	17.7167	15.2190
	Lamivudine	17.2692	18.4148	18.7463
	Zidovudine	-	-	-
1E7B	Tenofovir Disoproxil Fumarate	28.2644	25.0301	29.5930
	Tenofovir	17.4089	18.9333	19.8436
	Tenofovir alafenamide	26.8675	30.2668	28.8218
	Emtricitabine	17.9806	16.7575	16.5951
	Lamivudine	19.3115	19.2095	19.3580
	Zidovudine	-	-	-
1E7C	Tenofovir Disoproxil Fumarate	28.8152	28.9170	29.5264
	Tenofovir	21.4675	20.6283	20.3266
	Tenofovir alafenamide	31.7914	30.2244	36.1912
	Emtricitabine	16.5111	15.6657	18.1314
	Lamivudine	19.6171	18.1771	22.3318
	Zidovudine	-	-	-
1E7F	Tenofovir Disoproxil Fumarate	23.3718	30.4093	29.5706
	Tenofovir	20.2256	20.8013	20.5802
	Tenofovir alafenamide	30.1807	33.6850	33.3748
	Emtricitabine	18.3458	16.0368	18.2451
	Lamivudine	19.1614	17.7092	22.0348
	Zidovudine	-	-	-
1E7H	Tenofovir Disoproxil Fumarate	30.3385	28.8042	30.1009
	Tenofovir	17.9456	20,4324	19.7288
	Tenofovir alafenamide	30.8558	28.2569	33.8603
	Emtricitabine	16.2907	15.3676	18.3679
	Lamivudine	19.5995	17.1771	22.5623
	Zidovudine	-	-	-
1GNI	Tenofovir Disoproxil Fumarate	25.9416	28.8071	30.9970
	Tenofovir	19.2076	17.4202	19.9060
	Tenofovir alafenamide	27.3012	31.1437	33.8972
	Emtricitabine	17.4314	15.8174	18.0059
	Lamivudine	19.0245	16.9723	22.5487
	Zidovudine	-	-	-
1N5U	Tenofovir Disoproxil Fumarate	27.2337	32.1094	34.1769
	Tenofovir	17.4796	17.2055	20.8938
	Tenofovir alafenamide	27.9397	32.0147	34.3725
	Emtricitabine	15.9681	17.8598	17.8183
	Lamivudine	15.9598	18.7600	22.3153
	Zidovudine	-	-	-
2BXA	Tenofovir Disoproxil Fumarate	28.5506	25.8459	24.0071
	Tenofovir	18.3634	20.4800	18.3057
	Tenofovir alafenamide	27.7123	28.003	26.5800

2BXA	Emtricitabine	19.9651	15.9257	15.006
	Lamivudine	20.9481	18.9472	17.8932
	Zidovudine	-	-	-
2BXH	Tenofovir Disoproxil Fumarate	30.8008	27.4392	28.4176
	Tenofovir	17.4450	21.3432	18.3544
	Tenofovir alafenamide	25.8341	22.0179	29.3982
	Emtricitabine	18.0705	16.1844	16.6757
	Lamivudine	16.3022	19.0924	18.3171
	Zidovudine	-	-	-
2BXK	Tenofovir Disoproxil Fumarate	33.3196	31.2347	31.3942
	Tenofovir	20.0425	17.5773	20.8373
	Tenofovir alafenamide	35.9756	31.7153	33.8260
	Emtricitabine	19.7238	15.0405	18.2131
	Lamivudine	19.1428	18.3795	22.5863
	Zidovudine	-	-	-
2BXP	Tenofovir Disoproxil Fumarate	30.8116	28.7296	31.3275
	Tenofovir	17.6846	17.2087	20.6922
	Tenofovir alafenamide	29.4736	31.1541	33.7065
	Emtricitabine	20.8431	14.9107	17.6207
	Lamivudine	19.1518	17.9250	21.9303
	Zidovudine	-	-	-
2VUE	Tenofovir Disoproxil Fumarate	28.8484	27.2899	31.3242
	Tenofovir	18.1121	19.7062	19.4945
	Tenofovir alafenamide	26.5395	27.1462	34.1530
	Emtricitabine	17.9062	17.4483	17.3644
	Lamivudine	16.2899	18.5807	18.1454
	Zidovudine	-	-	-
2XWO	Tenofovir Disoproxil Fumarate	30.2173	25.7610	28.4605
	Tenofovir	20.1387	20.0937	17.3443
	Tenofovir alafenamide	32.1351	28.5499	30.3166
	Emtricitabine	20.8259	17.1934	15.5376
	Lamivudine	20.9819	18.7692	19.1491
	Zidovudine	-	-	-
4E99	Tenofovir Disoproxil Fumarate	30.3147	27.6619	25.5261
	Tenofovir	21.0474	19.1933	19.1997
	Tenofovir alafenamide	30.7600	22.0661	27.0124
	Emtricitabine	19.1853	14.4132	18.3865
	Lamivudine	20.8587	19.3279	15.7890
	Zidovudine	-	-	-
4L8U	Tenofovir Disoproxil Fumarate	36.4316	28.3305	33.5341
	Tenofovir	22.4935	16.8458	20.7925
	Tenofovir alafenamide	35.6027	32.7545	33.8098
	Emtricitabine	19.0081	14.8017	18.9780
	Lamivudine	20.4909	18.6138	20.0071
	Zidovudine	-	-	-
4L9K	Tenofovir Disoproxil Fumarate	26.4352	23.9595	28.8436
	Tenofovir	19.1356	15.8471	20.4657
	Tenofovir alafenamide	29.0239	24.6599	34.0372

|				
4L9K	Emtricitabine	17.3126	12.6429	17.7331
	Lamivudine	16.4008	14.5976	20.0691
	Zidovudine	-	-	-
4L9O	Tenofovir Disoproxil Fumarate	32.5174	26.2715	23.5035
	Tenofovir	20.4743	17.3709	18.7233
	Tenofovir alafenamide	33.2551	28.0290	27.7046
	Emtricitabine	17.6778	14.2754	13.4693
	Lamivudine	19.3463	19.2850	16.1619
	Zidovudine	-	-	-
6EZQ	Tenofovir Disoproxil Fumarate	29.1743	37.0220	26.6077
	Tenofovir	20.1956	21.9918	17.2980
	Tenofovir alafenamide	26.4699	32.2935	30.4390
	Emtricitabine	18.9956	17.6632	16.4967
	Lamivudine	19.8828	21.4175	20.1278
	Zidovudine	-	-	-
6HSC-	Tenofovir Disoproxil Fumarate	32.5510	30.5809	27.4068
	Tenofovir	21.4891	20.7867	23.0643
	Tenofovir alafenamide	34.6711	31.7968	24.8784
	Emtricitabine	18.6534	16.9636	17.8263
	Lamivudine	19.1718	18.2995	20.1591
	Zidovudine	-	-	-
6WUW	Tenofovir Disoproxil Fumarate	34.4513	31.1674	33.8268
	Tenofovir	22.5751	18.6330	20.8608
	Tenofovir alafenamide	25.9066	30.3981	36.4902
	Emtricitabine	16.8525	16.3741	19.6233
	Lamivudine	21.1824	18.7772	22.2002
	Zidovudine	-	-	-
Results		29	19	42
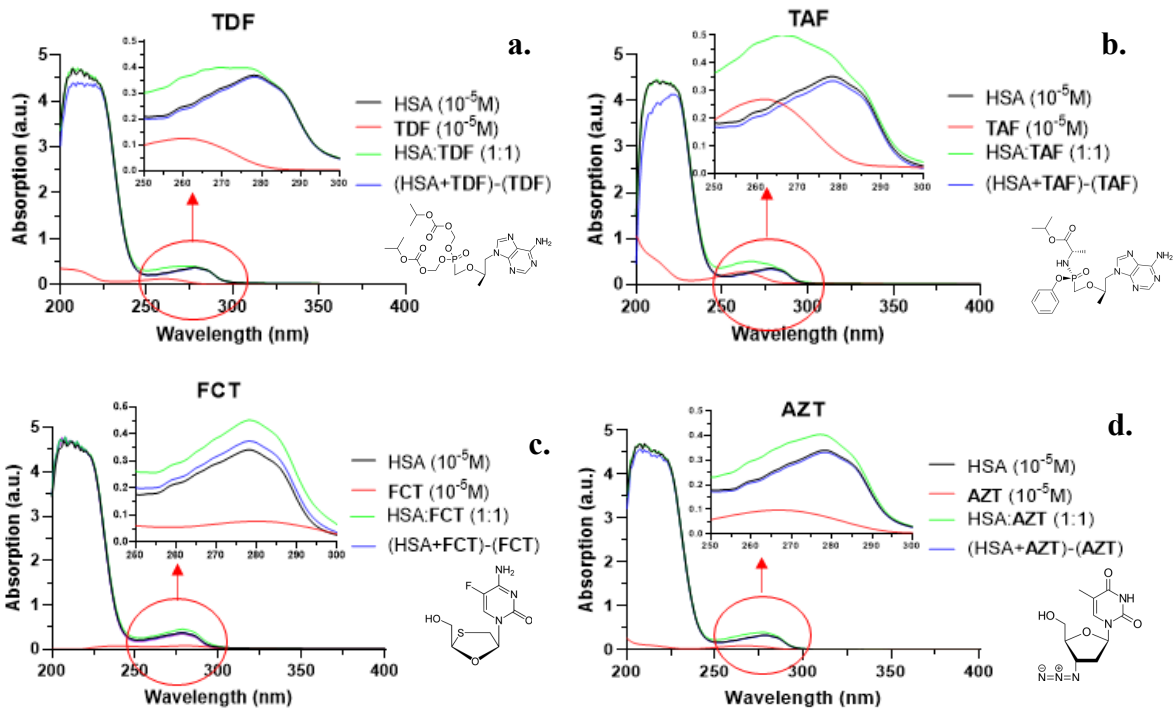
Figure 1. UV-VIS absorption spectra to HSA, HSA:TDF (1:1), and TDF (**a**), and HSA, HSA:TAF (1:1), and TAF (**b**), HSA, HSA:FCT (1:1), and 3TC (**c**), and HSA, HSA:AZT (1:1), and AZT (**d**)
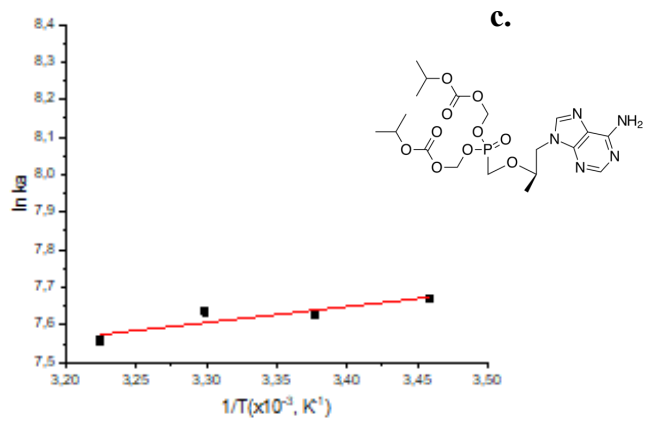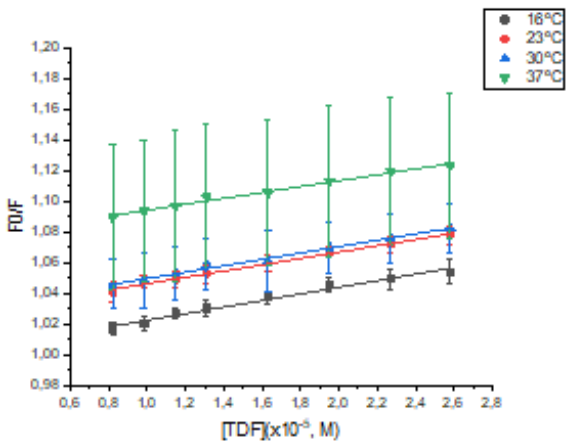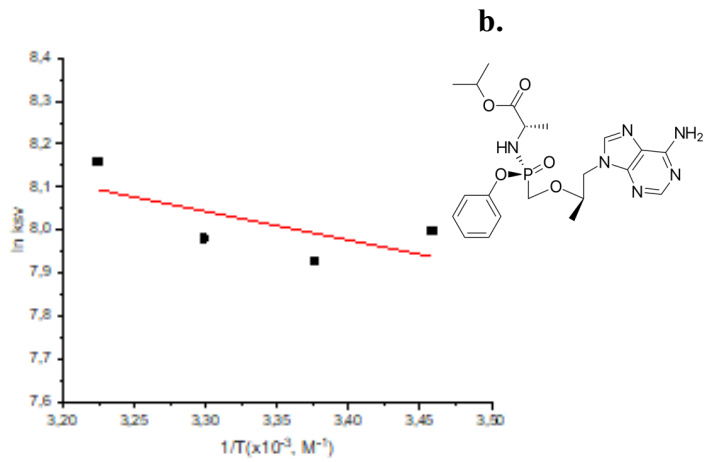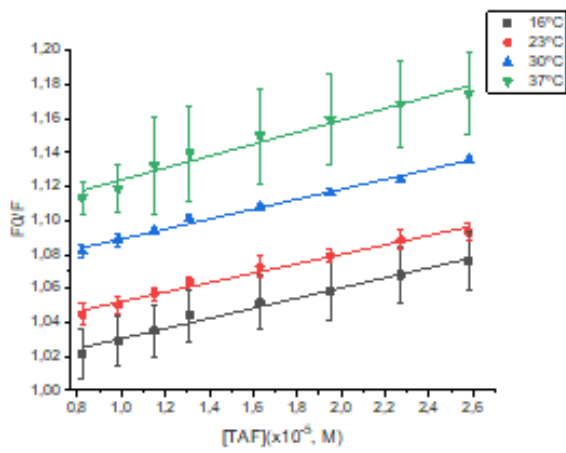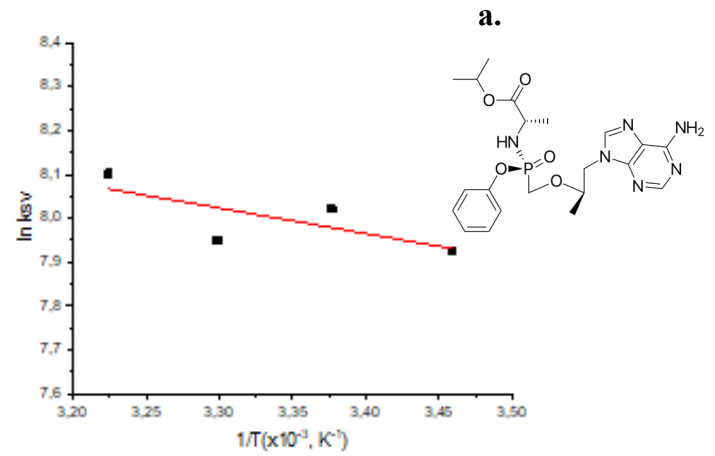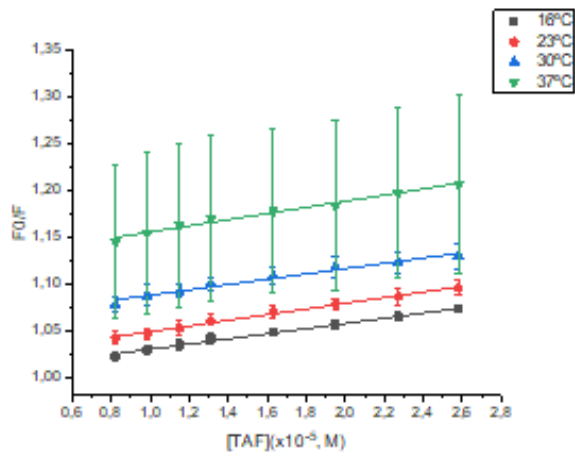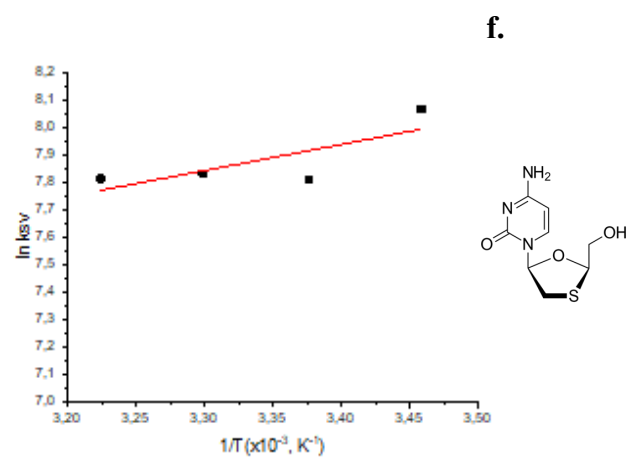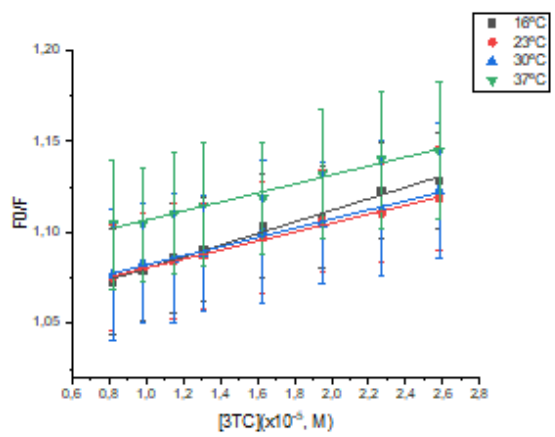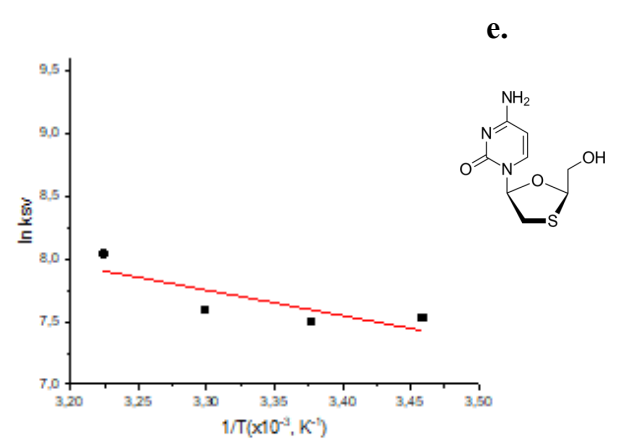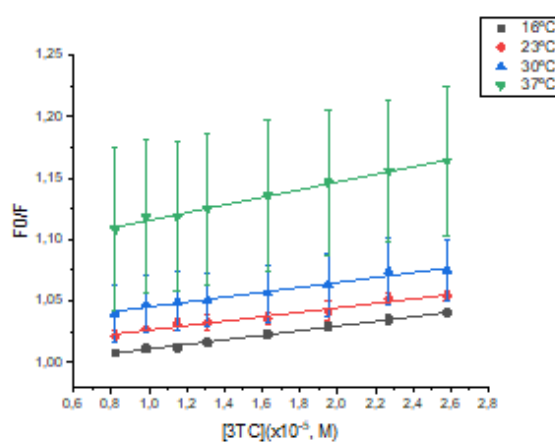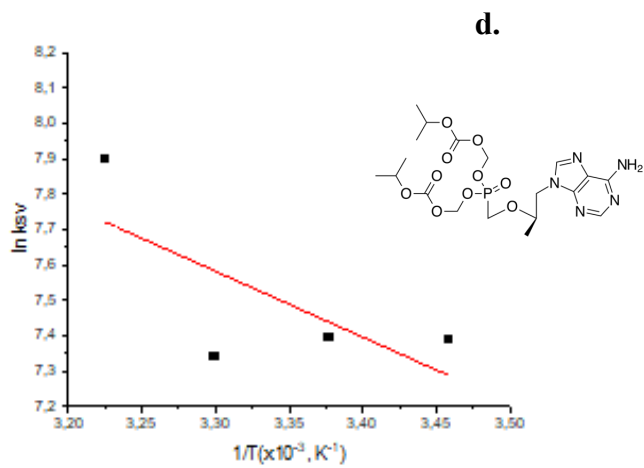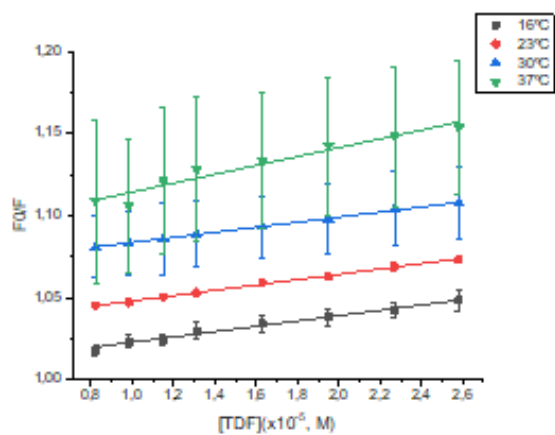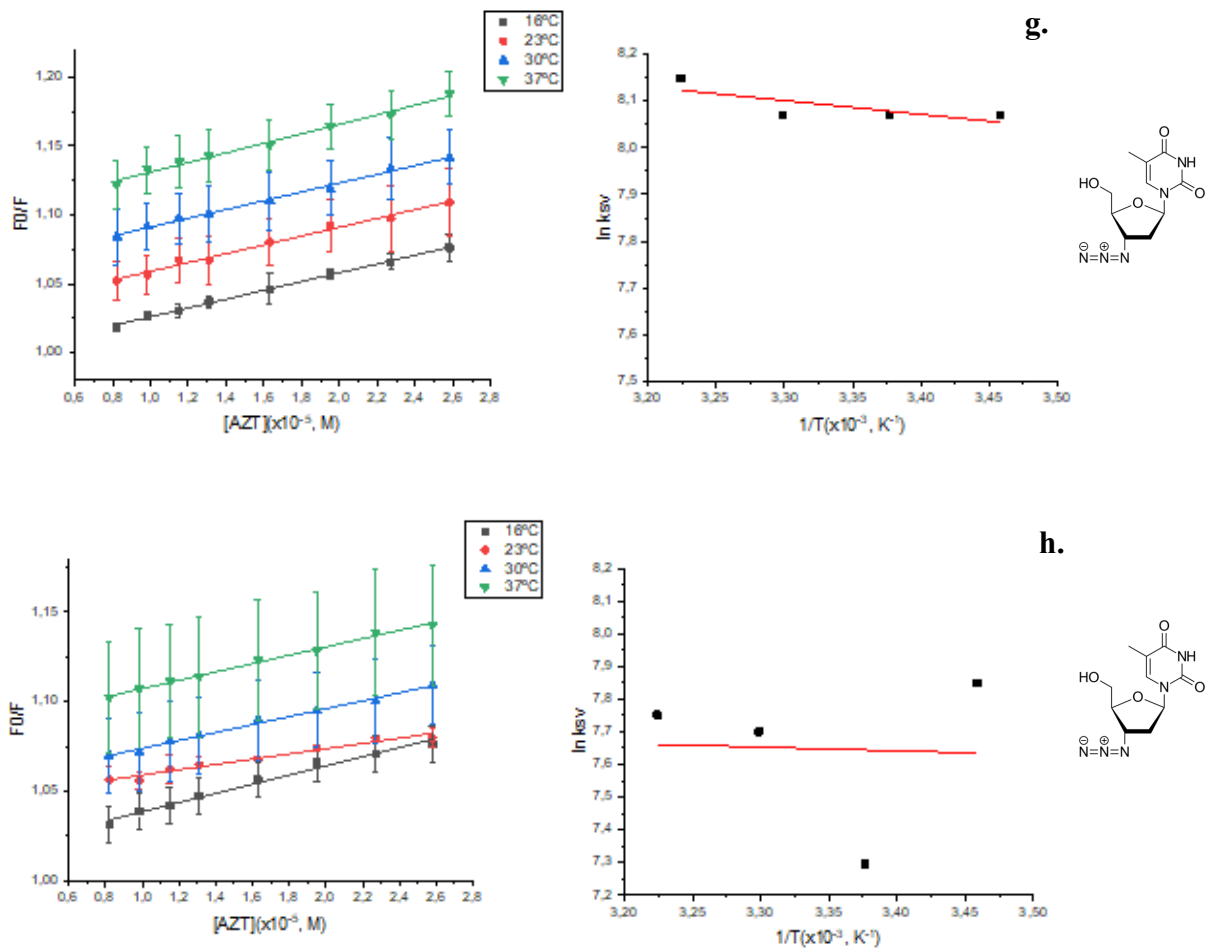
Figure 2. Stern-Volmer and Van Toff representations of TAF-HSA (**a**), TAF-BSA (**b**), TDF-HSA (**c**), TDF-BSA (**d**), 3TC-HSA (**e**), 3TC-BSA (**f**), AZT-HSA (**g**), AZT-BSA (**h**).
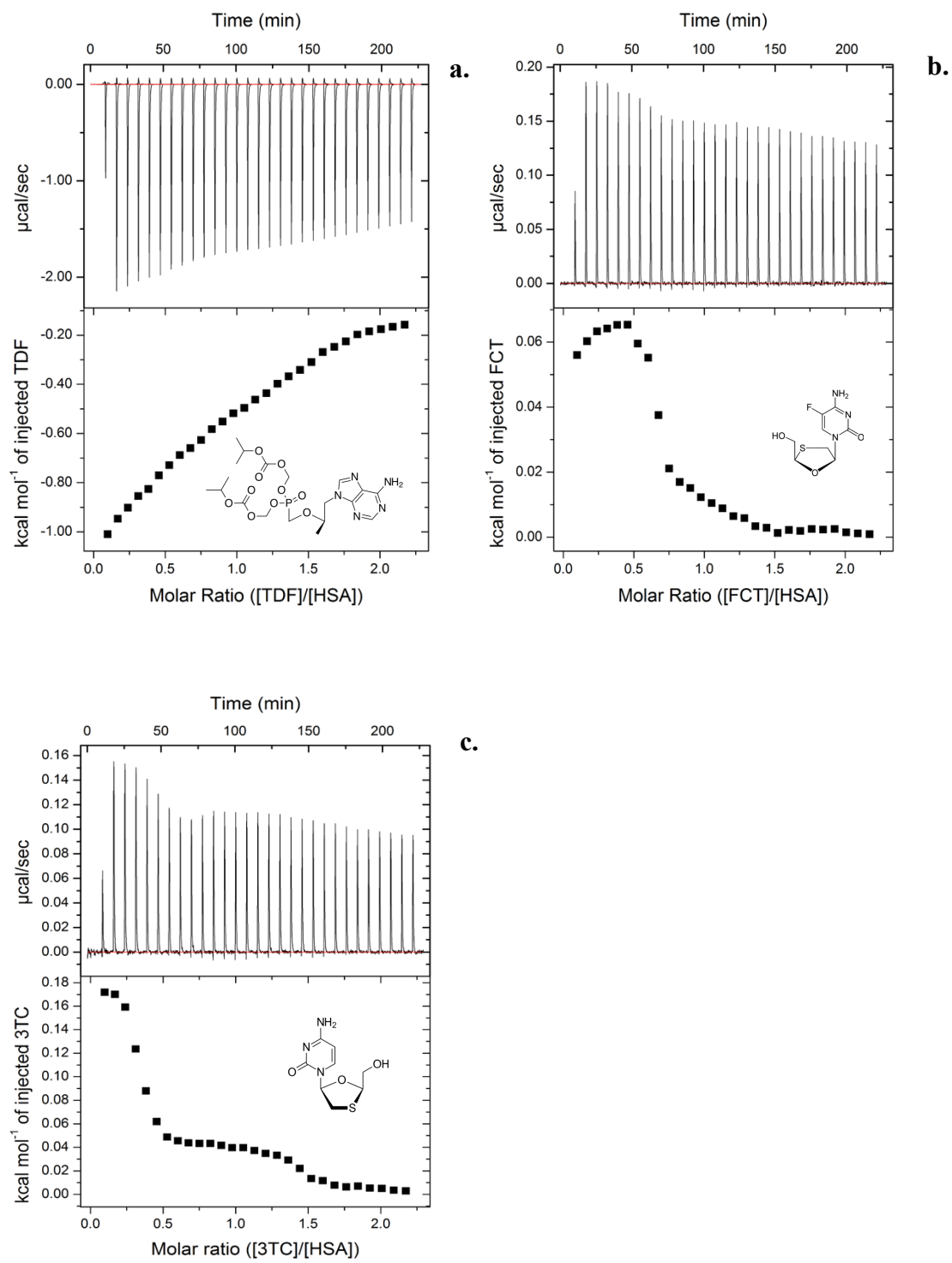
Figure 3. Calorimetry titration of TDF-HSA (**a**), FCT-HSA (**b**), and 3TC-HSA (**c**).